# Geometry and Temperature Effects on The Tensile Modulus of Randomly Oriented Short Fibers Reinforced Biocomposites Using Finite Elements Method

by

Farah NADDAF

THESIS PRESENTED TO ÉCOLE DE TECHNOLOGIE SUPÉRIEURE
IN PARTIAL FULFILLEMENT OF THE REQUIREMENTS FORTHE
DEGREE OF MASTER'S OF AEROSPACE INGENEERING WITH THESIS
M .A.SC.

MONTREAL, OCTOBER 18, 2023

ÉCOLE DE TECHNOLOGIE SUPÉRIEURE
UNIVERSITÉ DU QUÉBEC

**BOARD OF EXAMINERS THESIS M.A.SC**

**THIS THESIS HAS BEEN EVALUATED**

**BY THE FOLLOWING BOARD OF EXAMINERS**

Mr. Anh Dung Ngô, Thesis Supervisor
Department of Mechanical Engineering, École de technologie supérieure

Mr. Omar Chaalal, Chair, Board of Examiners
Department of Construction Engineering, École de technologie supérieure

Mr. Hakim Bouzid, Member of the jury
Department of Mechanical Engineering, École de technologie supérieure

THIS THESIS WAS PRENSENTED AND DEFENDED

IN THE PRESENCE OF A BOARD OF EXAMINERS AND PUBLIC

SEPTEMBER 28, 2023

AT ÉCOLE DE TECHNOLOGIE SUPÉRIEURE

## ACKNOWLEDGMENT

I would like to express my sincere gratitude to my research director, professor Anh Dung NGÔ for his invaluable guidance and support through my master's study. Without his help, this journey would not have been possible, and I would not be able to complete my research.

I would also like to thank the jury members who do me the honor to evaluate my thesis and providing helpful feedback and suggestions.

I am grateful to École de technologie supérieure, for providing me with the opportunity to conduct my research, and for all of the resources and support it provided.

I would also like to thank my husband Hani for his support during my study.

I dedicate my hard work to the light of my life, my heart Albi-Jolie.

Finally, I would like to thank all of the participants in my study for their time and willingness to share their experiences. This work would not have been possible without their contribution.

**L’effet de la géométrie et de la température sur le module tension de biocomposites renforcés par des fibres courtes à orientation aléatoire à l’aide de la méthode des éléments finis**

Farah NADDAF

## RESUMÉ

Dans cette étude, l'effet de la géométrie des fibres et de la température sur le module de traction des matériaux biocomposites est étudié. Le logiciel Digimat® est utilisé, qui applique la méthode des éléments finis en réalisant la modélisation numérique des biocomposites C1, C2, et du biocomposite (PP+30%Hemp).

Le premier matériau biocomposite modélisé C1 est constitué de la matrice (PHBV/PBAT) renforcée par 30 % en poids de fibres Switchgrass, tandis que le deuxième matériau biocomposite C2 est constitué d'une matrice de polypropylène (PP) renforcée avec 30% en poids de fibres Miscanthus.

Pour valider la précision des travaux actuels, une comparaison entre les résultats de modélisation menés et les résultats expérimentaux précédents est effectuée, et la possibilité d'évaluer le module de traction des biocomposites C1 et C2 en utilisant le logiciel Digimat® est confirmée.

En ce qui concerne l'effet des géométries des fibres, on constate que le facteur essentiel dans les fibres cylindriques est le ratio L/D. Lorsque la longueur des fibres augmente, le ratio L/D augmente, ce qui conduit à un module plus élevé. Le même motif est confirmé pour les fibres rectangulaires, lorsque la longueur des fibres rectangulaires augmente, cela conduit également à un module de traction plus élevé.

De plus, après une certaine valeur de longueur de fibre, le module de traction devient stable. Les résultats ont montré que le module de traction reste relativement constant après une certaine valeur de longueur de la fibre.

L'effet de la longueur de la fibre sur le module de traction des biocomposites a été discuté pour les fibres Miscanthus et le fibres Switchgrass à section cylindrique et rectangulaire, et dans les deux c’est le même schéma.

Pour l'effet de la température sur le module de traction des matériaux biocomposites, il est confirmé que le module de la matrice et des fibres diminue avec l'augmentation de la température, par conséquent le module du matériau composite diminue.

**Mots-clés:** Miscanthus, Switchgrass, homogénéisation numérique, géométries, température

**Geometry and temperature effects on the tensile modulus of randomly oriented short fibers reinforced biocomposites using finite elements method**

Farah NADDAF

## ABSTRACT

In this study, the effect of the fiber's geometry and the temperature on the tensile modulus of biocomposite materials is investigated. Digimat® software is used, which applies the numerical finite elements method to obtain the tensile modulus of the biocomposites C1, C2, and the biocomposite (PP+30%Hemp).

The first modeled biocomposite material C1 consists of (PHBV/PBAT) matrix reinforced by 30% of randomly oriented short natural Switchgrass fibers, while the second biocomposite material C2 is built of polypropylene (PP) matrix reinforced with 30% of randomly oriented short natural Miscanthus fibers.

To validate the approach, a comparison between the conducted modeling results and previous experimental results is done, and the possibility to evaluate the tensile modulus of the biocomposites C1 and C2 by using Digimat® software is confirmed.

Regarding the effect of fiber geometries, it is found that the essential factor in cylindrical fibers is the ratio L/D. When the length of the fibers increases, the ratio L/D increases, and this leads to a higher modulus. The same pattern is confirmed for the rectangular fibers, when the length of the rectangular fibers increases, it also leads to a higher tensile modulus.

Additionally, it is noticed that after a certain value of fiber length, the tensile modulus becomes stable. The results show that the tensile modulus remains relatively constant after a certain value of fiber length.

The effect of the fiber length on the tensile modulus of biocomposites was discussed for both Miscanthus and Switchgrass fibers with cylindrical and rectangular cross-section, and follows the same pattern for both uses.

As for the effect of temperature on the tensile modulus of biocomposite materials, it is confirmed that the modulus of both matrix and fibers decreases with increasing temperature, consequently the modulus of the biocomposite material reduces.

**Keywords:** Miscanthus, Switchgrass, numerical homogenization, geometries, temperature

**TABLE OF CONTENTS**

Page

## LIST OF TABLES

Page

## LIST OF FIGURES

Page

## LIST OF ABREVIATIONS

| | |
|---|---|
| CAE | Computer-Aided Engineering |
| CPU | Central processing unit |
| PBAT | Poly (butylene adipate-co-terephthalate) |
| PHBV | Poly (3-hydroxybutyrate-co-3-hydroxyvalerate) |
| POE | Elastomers of Polyolefine |
| PP | Polypropylene |
| RVE | Representative Volume Element |
| $v_f$ | The volume content of the fibers in the composite |
| $\rho_f$ | The density of the fibers |
| $\rho_c$ | The density of the composite material |

## LIST OF SYMBOLS AND UNITS

**SYMBOLS**

| | |
|---|---|
| C1 | First studied biocomposite consists of (30wt% SG+ PHBV/PBAT) |
| C2 | Second studied biocomposite consists of (30wt% MS+ PP) |
| SG | Switchgrass short fibers |
| MS | Miscanthus short fibers |
| L | Length of the fibers |
| D | Diameter of the fibers |
| E | Tensile modulus |
| E1 | Young's modulus of the composite along the axis 1 |
| E2 | Young's modulus of the composite along the axis 2 |
| $E_{11}$ | Longitudinal Young's modulus |
| $E_{22}$ | Transverse Young's modulus |
| $E_m$ | Young's modulus of the matrix |
| $C_{ii}$ | The components of the stiffness matrix |

**UNITS**

| | |
|---|---|
| mm | Millimeter |
| g/$cm^3$ | Gram per cubic centimeter |
| MPa | Megapascal |
| GPa | Gigapascal |
| °C | Celsius degree |

# INTRODUCTION

Composite materials are considered an essential point of influence in several industries, including the automotive, aerospace, and naval sectors. They became popular because of their excellent mechanical properties and their lightweight. Many environmental concerns have caused a decrease in the use of products derived from fossil fuels. Moreover, lighter materials with a lower carbon content are required to reduce greenhouse emissions. Thus, more environmentally friendly materials like biocomposite materials are increasingly replacing the common composite materials.

This work uses the finite elements approach to study randomly oriented short natural fibers reinforced biocomposite materials. It seeks to find a numerical method to replace the empirical techniques in studying the effect of fiber geometry and temperature on the tensile modulus of biocomposite materials. The study investigates also the impact of temperature on the behavior of biocomposite materials reinforced by randomly oriented natural fibers.
Two biocomposites are modeled by using the approach of numerical homogenization:
-The first biocomposite C1 is a build-up of PHBV/PBAT matrix reinforced with 30wt% of randomly oriented short Switchgrass fibers.
- The second biocomposite C2 is a polypropylene matrix (PP) reinforced with 30wt% of randomly oriented short Miscanthus fibers.

The thesis covers three chapters,
-The first chapter covers the literature review of composite materials modeling, that includes the semi-empirical models, the analytical models, and the numerical models.
Due to the lack of data needed for developing the analytical model and the limited application of semi-empirical model, it is decided to use the numerical approach for this study.
In addition, it explains the representative volume element RVE, the boundary conditions, and discusses the method of finite elements. This section also explains the impact of the fiber geometries on tensile modulus of biocomposites. Finally, bibliographical review on the thermal effect on the mechanical properties of the matrix, the fibers, and the biocomposite (Hemp/PP).

-The second chapter presents the procedure for calculating the tensile modulus of two biocomposite materials. Under different fibers geometries form and it develops the numerical tools followed to characterize the tensile modulus for different forms of fibers under different temperature conditions using Digimat® commercial software.

-The third chapter illustrates the results of the numerical modeling by comparing the mechanical properties of two biocomposites, taking into consideration the following parameters (the reinforcement type, the shape, and the effect of temperature).

-Lastly, the conclusion and suggestions for future study are presented at the end.

# CHAPTER 1

# LITERATURE REVIEW

## 1.1 Introduction to bio composite materials

A composite is a combination of two or more separate materials. New composite materials such as fibres-reinforced-plastics consisting of reinforcing fibers embedded in a matrix or polymer binder are used more and more nowadays to replace metals, due to their higher specific stiffness and strength. In many applications, discontinuous or randomly oriented short fibers composites are the materials of choice because of the advantages of low cost, ease of fabricating complex parts, and isotropy. Figure 1.1 presents a schematic presentation of the constituents materials of a composite (Nagarajan, 2012).

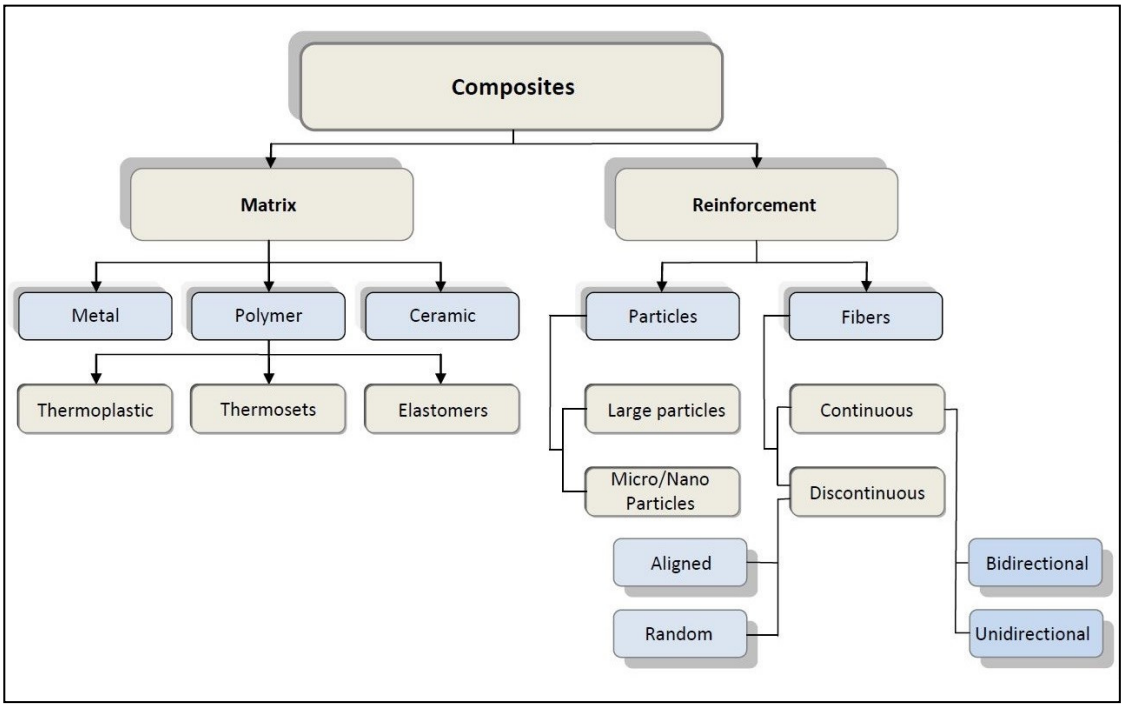


Figure 1.1 Classification of composite constituents

From Nagarajan (2012, p. 2)

Recently, as eco-friendly materials, a new class of composites known as biocomposites, made from natural fibers and petroleum based non-biodegradable polymers or biopolymers has been developed to answer the need of automotive industries. Figure 1.2 presents a schematic presentation of the definitions of biocomposite materials (Nagarajan, 2012).

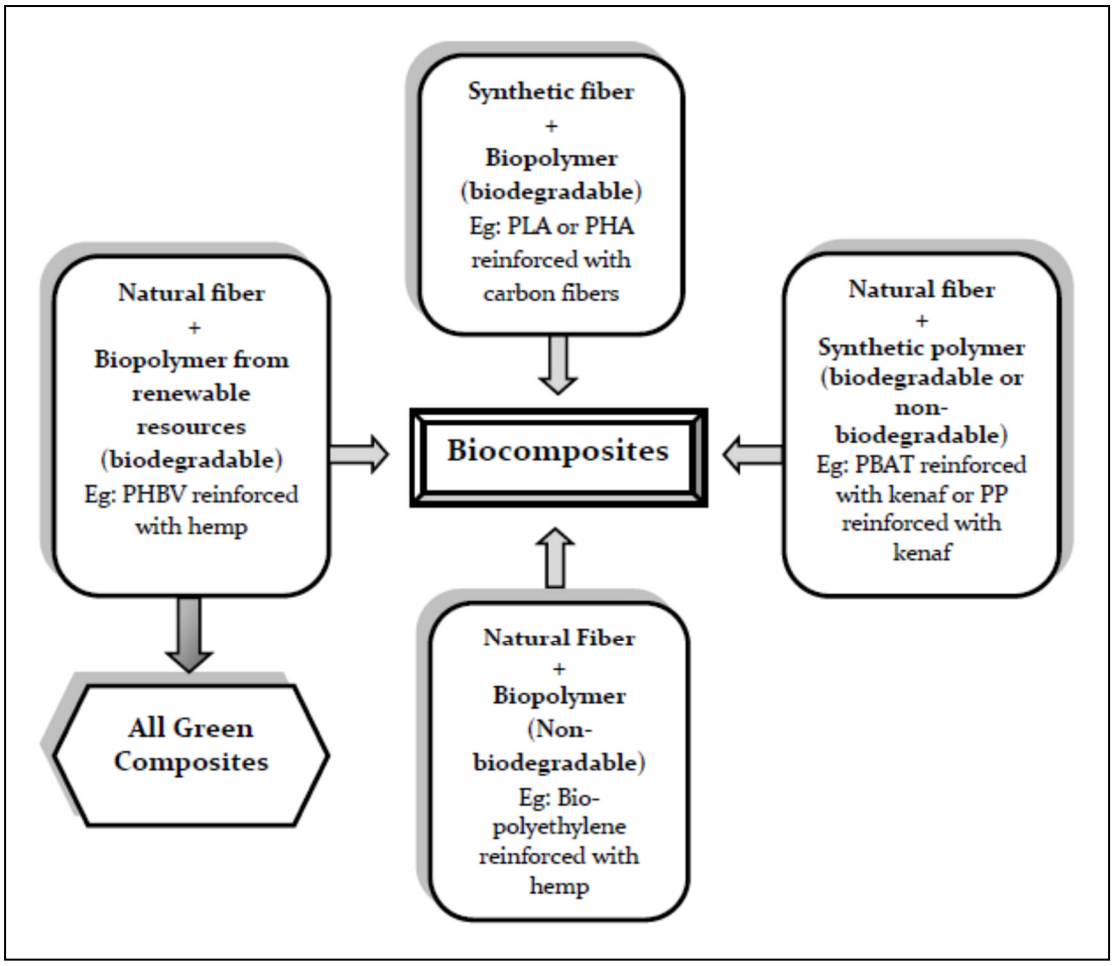


Figure 1.2 Terminology of biocomposites

From Nagarajan (2012, p. 12)

To produce an efficient structural composite, selecting specific fiber and matrix materials must be chosen carefully to avoid fiber breakage and matrix cracking. To develop a new composite, one has to understand the factors that influence its mechanical behavior and how to design it under service conditions and the manufacturing process. Besides experimentation, it is well

known that modeling is the most economical way to determine the optimum performance of the new product.

Materials derived from natural sources are referred to as bio-materials. These origins could be descended from plants or animals. Additionally, any substance made from a renewable source might be referred to as bio. At least one bio phase exists in the composition of biocomposite materials, which may also contain a natural matrix or natural reinforcements.

Due to their abundant resources and the simplicity of disposing of natural materials, these materials are more appealing. However, because these environmentally friendly composites do not require an industrial process to make them, they assist in lowering the CO2 emissions, which are steadily rising every day because of industries.

### 1.1.1 Biopolymers

Biopolymers have become more superior to synthetic polymers in terms of being environmentally friendly. However, their higher prices compared to conventional polymers pose a significant limitation. The behavior of polymers varies; some are flexible as rubber others are hard as Epoxy. Polymers take a considerable place in modern life; most are known as plastic materials which can be found anywhere in life.

Polymers may be divided into two groups: natural polymers, like rubber and bioplastic, and synthetic polymers, or plastics. Biopolymers are frequently employed as matrix or enhancement materials to increase specific matrix properties. Industry demand for biopolymers has increased due to their ease of extraction from nature and few adverse environmental effects.

### 1.1.2 Natural short fibers

The second crucial component or phase in the composite material is the fibers, due to their higher stiffness and strength. Therefore, the final composite material mechanical properties are enhanced by combining the fibers and matrix.

The two categories of fibers include synthetic and natural fibers. Industrial processes produce synthetic fibers like glass, spandex, and aramids using essential chemical ingredients. The second type consists of natural fibers, which comprise fibers extracted from natural sources; these are preferred over their industrial counterparts due to the following advantages:

- Lower cos
- Ease of processing
- Biodegradability
- Abundance

Natural resources are renewable and found all around, and they cause the least harm to the environment. Therefore, the goal of discovering natural alternatives to synthetic fibers is to maintain the lowest possible pollution rate in industry and development. Natural fibers, also known as bio-fibers, are the ideal alternatives for synthetic fibers since they can execute their function in composite materials while satisfying environmental preservation standards (K.Mohanty, A., Misra, M. & T.Drzal, 2006). Figure 1.3 shows the classification of natural fibers.

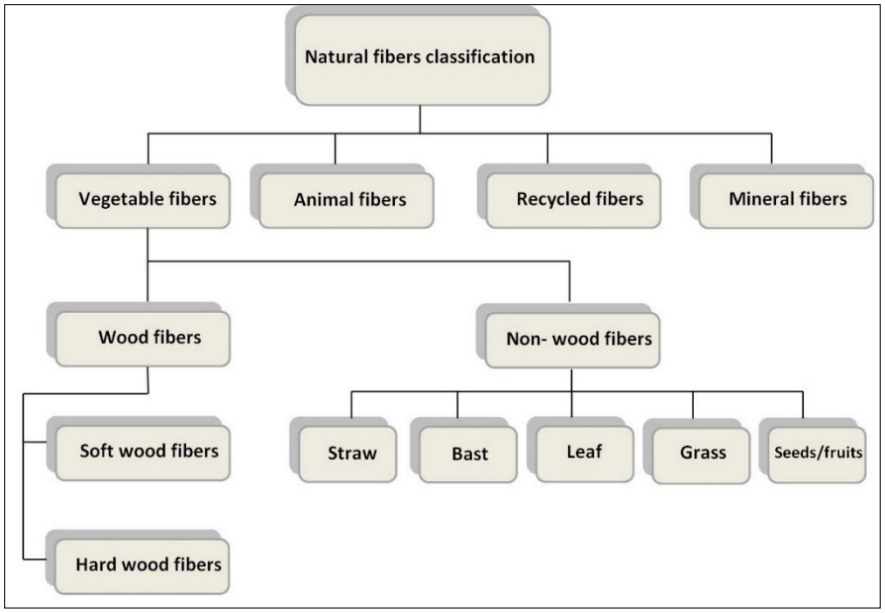


Figure 1.3 Classification of natural fibers

From Nagarajan (2012, p. 7)

## 1.2 Mechanical behavior modeling methods

There are three types of modeling: analytical, semi empirical and numerical using the finite elements method,

- Analytical model.
- Semi empirical models.
- Numerical models.

### 1.2.1 Micro - Macro analysis level

The two scales microscopic and macroscopic analyses are needed for modeling the effective modulus of heterogeneous material whose microstructure phase consists of a matrix material and inclusions such as short fibres or platelets etc.., subjected to a given loading boundary conditions. Micromechanics determine the behaviour of the composite material under the interaction of the constituent materials in considering their mechanical properties. Macro mechanical behaviour can be characterised as average stresses and strains as well as effective

mechanical properties in an equivalent homogeneous material. The concept of representative volume element RVE which should be large enough to represent the underlying microstructure and small with respect to the size of the solid body, helps to permit the transition between two scales. Figure 1.4 shows the transition process between micro and macro scales.

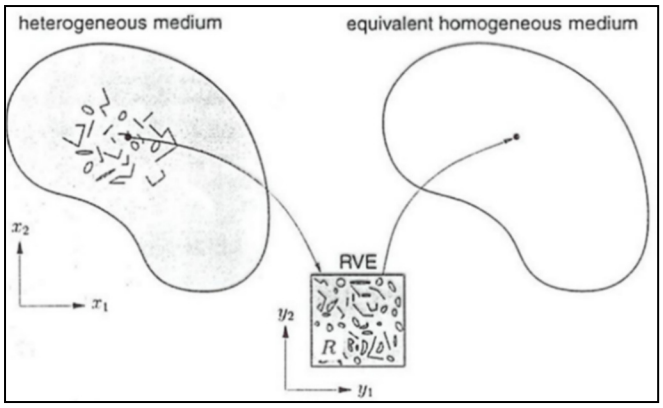


Figure 1.4 Micro-macro transition

From Digimat manual (2020, p. 243)

The process for modeling of short fibres composites starts with the analysis of the behaviour of the aligned short fibres, followed by the off-axis modeling and completed with randomly oriented reinforcement. Figure 1.5 shows different types of short fibers.

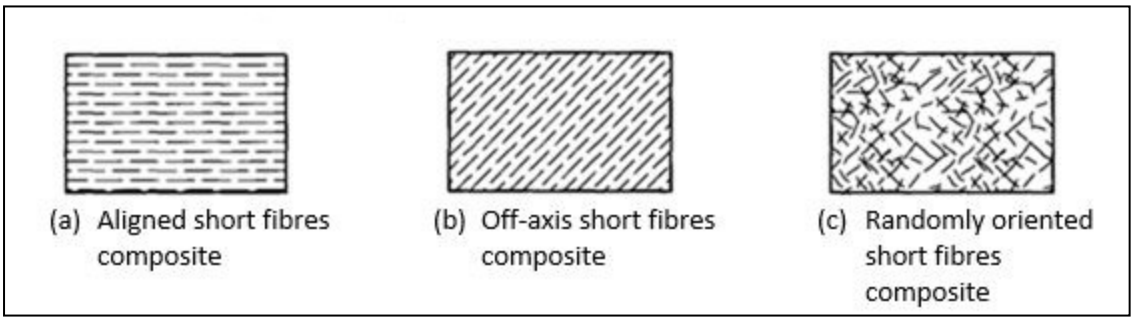


Figure 1.5 Types of short fibers

From Gibson (2016)

### 1.2.2 Fiber volume content

The volume content of the fibers in the composite is:

$$v_f = V_f / V_c \tag{1.1}$$

The density of the fibers and the density of the composite:

$$\rho_f = W_f / V_f \quad , \quad \rho_c = W_c / V_c \tag{1.2}$$

The volume content of the fibers:

$$v_f = \frac{W_f \times \rho_f}{W_c \times \rho_c} \tag{1.3}$$

Or the weight content of the fiber in the composite is:

$$w_f = \frac{W_f}{W_c} \tag{1.4}$$

$$\rightarrow w_f = (\rho_c / \rho_f) \times v_f \tag{1.5}$$

Thus:

$$\rightarrow w_f\% = (\rho_c / \rho_f) \times v_f\% \tag{1.6}$$

In the case of $\rho_c \approx \rho_f$ ;

$$w_f = v_f \tag{1.7}$$

Where:

$\rho_c$ : Represents the density of the composite.

$\rho_f$ : Represents the density of the fibers.

$V_f$: Represents the volume fraction of fibers.

$V_c$: Represents the volume of the composite.

$W_c$: Represents the weight of the composite.

$W_f$: Represents the weight of the fibers.

$v_f$: Represents the volume content of the fibers.

$w_f$: Represents the contents by weight of the fibers.

### 1.2.3 Aligned short fibers reinforced composites

#### 1.2.3.1 Analytical models

Figure 1.6 shows the RVE for the analysis of aligned short fibre composites.

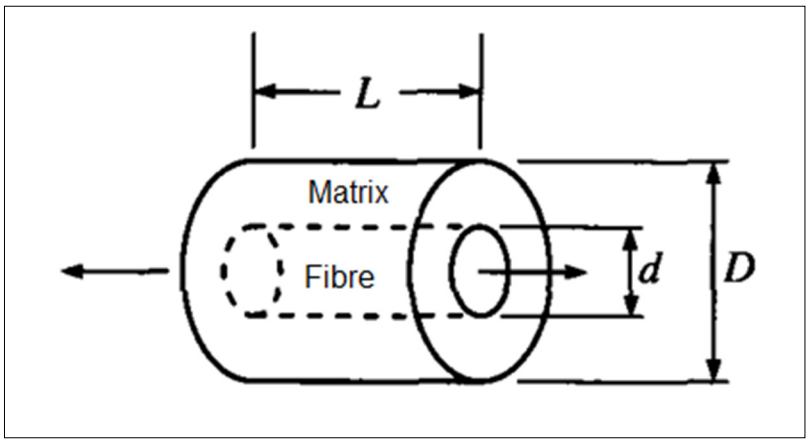


Figure 1.6 RVE for aligned short fibre composite
From Cox (1952)

Considering static equilibrium of the forces along the longitudinal (x) direction in the model presented in Figure 1.6 the fibre stress ($\sigma_f$) along this direction is related to the interfacial shear stress ($\tau$) as Equation (1.8):

$$\sigma_f = \frac{4}{6}\int_0^x \tau \, dx \tag{1.8}$$

The longitudinal axial modulus of the aligned short fibre composite has been established first by Cox, who assumed firstly that the interfacial shear stress is proportional to the difference between the axial displacement (u) at a point in the fibre and the displacement (v), that the matrix would have at the same point in the model without the present of the fibre. Secondly, by taking in to account the rule of mixture for stress that is valid for the RVE, the expression for the modulus was found as followed Equation (1.9) (Gibson, 2016):

$$E_{c_1} = E_{f_1}\left[1 - \frac{\tan(\beta L/2)}{\beta L/2}\right] v_f + E_m v_m \tag{1.9}$$

Where $G_m$ is the matrix shear modulus, Equation (1.10) from (Gibson, 2016):

$$\beta^2 = \frac{2\pi G_m}{A_f E_{f1} \ln\left(\frac{D}{d}\right)} \tag{1.10}$$

#### 1.2.3.2 Semi-empirical models

**Halpin-Tsai :**

Equation (1.11) from (Gibson, 2016):

$$\frac{E_2}{E_m} = \frac{1 + x_2\, h_2\, u_f}{1 - \, h_2\, u_f} \tag{1.11}$$

Where $\xi$=2 for $v_f$= 0.55, and:

$$\eta_2 = \frac{(\frac{E_{f2}}{E_m} - 1)}{(\frac{E_{f2}}{E_m} + \xi_2)} \tag{1.12}$$

**Halpin:**

In order to introduce the geometric parameter ($\xi$1 ) Halpin suggested to the adapt the (Halpin & Tsai, 1967) as followed:

$$\frac{E_1}{E_m} = \frac{1 + x_1\, h_1\, u_f}{1 - \, h_1\, u_f} \tag{1.13}$$

$$\eta_1 = \frac{(\frac{E_{f1}}{E_m} - 1)}{(\frac{E_{f1}}{E_m} + \xi_1)} \tag{1.14}$$

$$\xi_1 = \frac{2\, L}{d} \tag{1.15}$$

Where L and d are the fiber length and diameter.

### 1.2.3.3 Numerical models

(Gibson, 2016) studied the effect of fibre end gap on the composite modulus by using finite elements model. Figure 1.7 shows a good agreement between predictions from both finite elements model with experimental data.

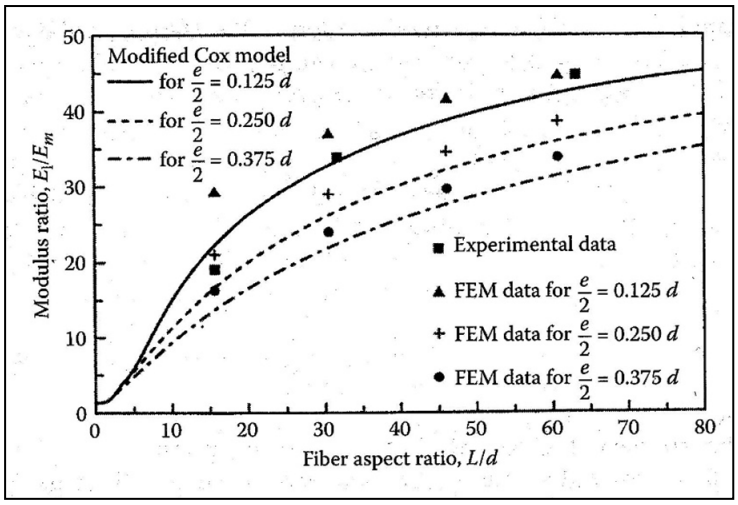


Figure 1.7 Predictions for both finite elements model with experimental data From Gibson (2016)

### 1.2.4 Off-axis modulus of aligned short fibers reinforced composites

(Sun et al., 1985) and (Suarez et al., 1986) suggested that the off-axis modulus of the short fibre composite ($E_x$) may be calculated by substituting the Cox model equation to calculate the longitudinal modulus $E_1$, the transverse modulus $E_2$, the in-plane shear modulus $G_{12}$ and the major Poisson's ratio. Figure 1.8 shows a comparison of the predicted off-axis modulus $E_x$, for graphite/epoxy composite with experimental values.

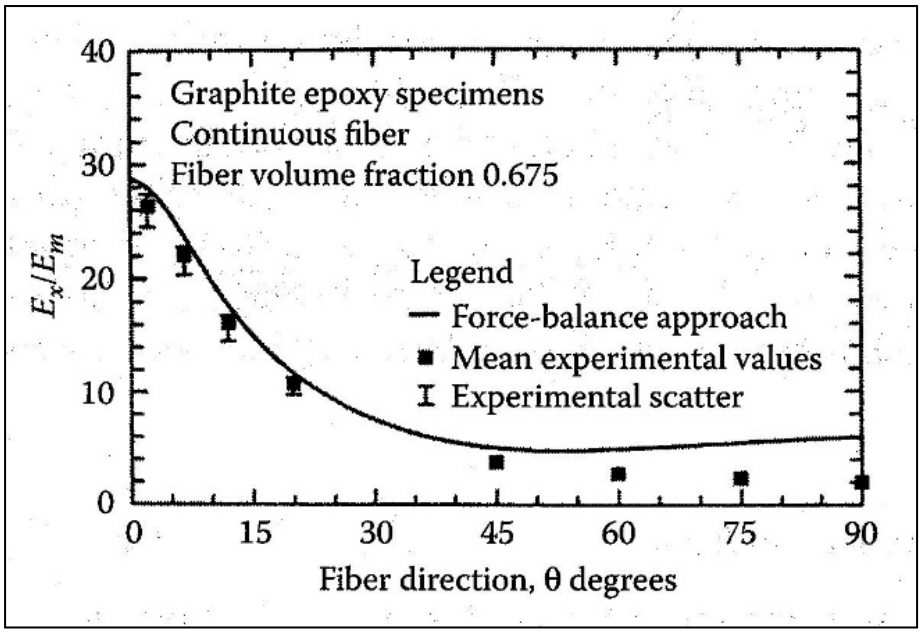


Figure 1.8 The predicted off-axis modulus $E_x$, for graphite/epoxy composite with experimental values.

From Gibson (2016)

### 1.2.5 Randomly oriented short fibers reinforced composites

#### 1.2.5.1 Analytical models

By modeling a paper as planar mat continuous fibre Cox has also introduced the concept of averaging the elastic modulus over all possible fibre direction by integration. The results are not considered sufficiently accurate for the design use.

(Tsai & Pagano, 1968) and (Halpin & Pagano, 1969) have used the invariants concept along with quasi-isotropic laminate theory to develop the following equations for the estimation of average properties of randomly oriented short fibre composites:

$$\tilde{E} = \frac{(U_1 - U_4)(U_1 + U_4)}{U_1} \tag{1.16}$$

$$\tilde{G} = \frac{(U_1 - U_4)}{2} \quad (1.17)$$

$$\tilde{V} = \frac{U_4}{U_1} \quad (1.18)$$

Where $U_1$ and $U_4$ are the invariants calculated from the mechanical constants $E_1$, $E_2$, $G_{12}$ and $\nu_{12}$ for a continuous fibre equivalent lamina. These models have considered only the fibre orientation without the fibre length effect. On the other hand, the data on the mechanical properties of the PHBV-PBAT/Switchgrass and Miscanthus/PP are not available in the literature.

#### 1.2.5.2 Semi-empirical models

(Tsai & Pagano, 1968) has suggested the approximation expression where the $E_{11}$ and $E_{22}$ are calculated using the relation for aligned short fiber composites:

$$E_{random} = \frac{3}{8} E_{11} + \frac{5}{8} E_{22} \quad (1.19)$$

Calculating $E_{11}$ and $E_{22}$ using the Halpin-Tsai equation for unidirectional fibers composite materials is possible. Moreover, this equation considers the influence of the ratio L/t and L/d.

- The longitudinal modulus $E_{11}$ is calculated by the Equation (1.20):

$$E_{11} = \frac{1 + \zeta_1 \, \eta_L \, v_f}{1 - \eta_L \, v_f} E_m \quad (1.20)$$

$$\eta_L = \frac{(\frac{E_f}{E_m} - 1)}{(\frac{E_f}{E_m} + \zeta_1)}$$

$$\zeta_1 = \frac{2\,L}{d}$$

L: Represents the length of the fibers; d: represents the diameter of the fibers.

- The transverse modulus $E_{22}$ is calculated by the equation of (Halpin & Tsai, 1967)

$$E_{22} = \frac{1 + \zeta_2 \, \eta_T \, v_f}{1 - \eta_T \, v_f} E_m \tag{1.21}$$

$$\eta_T = \frac{(\frac{E_f}{E_m} - 1)}{(\frac{E_f}{E_m} + \zeta_2)}$$

$\zeta_2$: Represents a parameter that refers to how much the fibers reinforce the matrix. As a function of the component stiffness ratio $E_f/E_m$, it corresponds to the curve-fitting parameter that reflects the normalized transverse stiffness $E_{22}/E_m$.

Most of the time, semi-empirical models do not provide precise forecasts since they only account for some of the microstructure's information (the properties of the phases, their volume fraction, the shape, and the orientation of the reinforcements). Furthermore, they do not serve as models that explain physical occurrences.

#### 1.2.5.3 Numerical models

**Representative Volume Element RVE**

In the literature, RVE is defined in many ways. For example, there have been several definitions of RVEs that consider the morphology of the microstructure or its physical characteristics. RVE stands for Representative Volume Element, which refers to a sample volume of a material with a microstructure representing the material as a whole. The RVE

contains enough information about the microstructure to make predictions about the macroscopic behavior of the material.
By studying the behavior of the RVE under certain conditions, such as displacement or stress, it is possible to determine the material's macroscopic properties, such as its stiffness or strength. The key feature of the RVE is that it must be large enough to capture the essential features of the microstructure but small enough to be analyzed using computational methods (Hill, 1963).

The RVE is a small representative volume of a material that makes it possible to determine its valuable properties. By analyzing the behavior of this sample under different loading conditions, we can determine the material macroscopic properties, such as its modulus of compressibility.

Using the RVE approach to determine the modulus of compressibility helps accurately model the material's behavior in larger-scale applications and it ensures that it performs as expected under different loading conditions (Gusev, 1997).

The researchers tried optimizing their calculations and production time using Representative Volume Elements (RVEs) with the smallest feasible size. However, in some cases, tiny quantities may only partially achieve the RVE with a small volume. To address this issue, researchers can use a representational Elementary Volume (EV) with an acceptable margin of error.

To define the RVE, researchers often model several volume values and compute effective properties. (Kanit et al., 2003) proposed a standard that considers the average value and deviation of the modeled property based on many modeling attempts. This standard aims to establish how many attempts are needed to ensure a certain level of precision and is known as the confidence criteria (Kanit et al., 2003) (Lu, Z., Yuan, Z. & Liu, 2014).

These approaches can help researchers to model materials and properties accurately while minimizing calculation and production times.

$$\varepsilon_{rela} = \frac{\varepsilon_{abs}}{Z} = \frac{2D_z\,(V)}{Z\sqrt{n}} \tag{1.22}$$

- $Z$ Is the average value of the estimated property.
- $D_z\,(V)$ Is the standard deviation of the property.
- n Is the number of realizations.

The modulus E1 and E2 were used to replace the parameter "Z" while applying the confidence criteria. The RVE guarantees the assumption of planar isotropy. For materials with transverse isotropic behavior, it is necessary to verify the isotropy of the RVE. In the literature, a criterion for testing the initial isotropy involves evaluating the degree of isotropy of the elementary volume. This initial isotropy criterion and a confidence criterion have been used in several studies to determine the appropriate size of the RVE (Lu, Z., Yuan, Z. & Liu, 2014).
It is calculated by the following Equation (1.23):

$$\Delta = \sqrt{(\Delta_1{}^2 + \Delta_2{}^2)} \text{ when } \Delta_1 = \frac{2(C_{11} - C_{22})}{C_{11} + C_{22}},\ \Delta_2 = \frac{2(C_{11} - C_{12} - 2\,C_{66})}{C_{11} + C_{22} + 2\,C_{66}} \tag{1.23}$$

For planar isotropy materials, $\Delta$ equals zero.
$C_{ii}$: The components of the stiffness matrix.
The acceptable RVE is considered when the value of $\Delta$ does not exceed 5%.

**Boundary conditions**

When calculating the RVE, the boundary conditions are the crucial factor (Kanit et al., 2006). It has been demonstrated in several papers that the RVE can be reached more quickly under some boundary conditions than others.

a) Dirichlet boundary conditions,

It is often known as the boundary conditions limits of deformations since they are determined by the subjugation of displacements on the surfaces of the elementary volumes. The boundary conditions distribution is applied on two surfaces of the elementary volume as an illustration for straightforward traction. The second surface is displaced while the first remains stationary. Every face of the VE that does not experience deformations is subjected to a constant deformation distribution. Figure 1.9 shows Dirichlet boundary condition

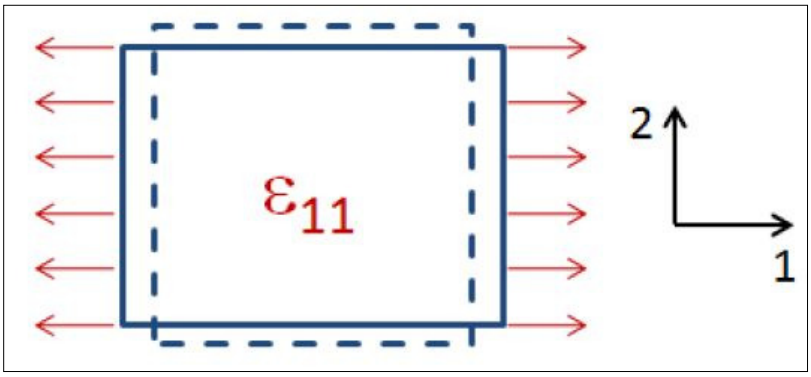


Figure 1.9 Dirichlet boundary Conditions

From Digimat manual (2020, p. 641)

b) Mixed boundary conditions,

Under these boundary conditions, not all elementary volumes surfaces get a displacement field. Whenever two surfaces have a displacement field applied to them while the other surfaces are left free (E-Xstream, 2020). Figure 1.10 shows the mixed boundary condition.

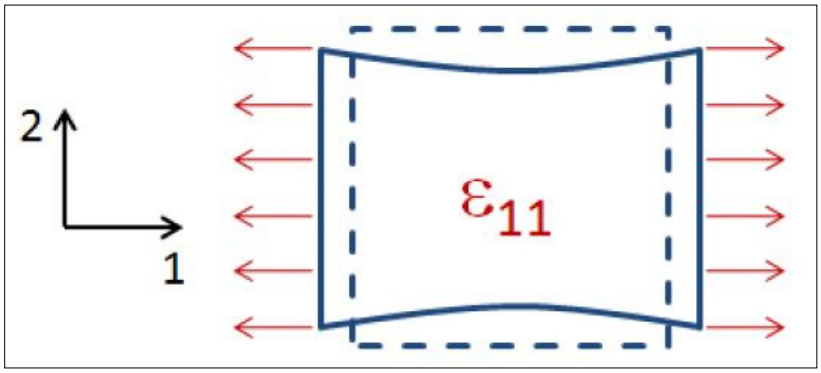

Figure 1.10 Mixed boundary conditions
From Digimat manual (2020, p. 641)

c) Periodic boundary conditions,

These boundary conditions are not limited to periodic geometry. Although applying a displacement to a surface is summed by a displacement fluctuation function, the idea is nearly identical to Dirichlet boundary conditions. Periodically, this oscillation occurs between the representatives faces. Figure 1.11 shows the Periodic boundary condition.

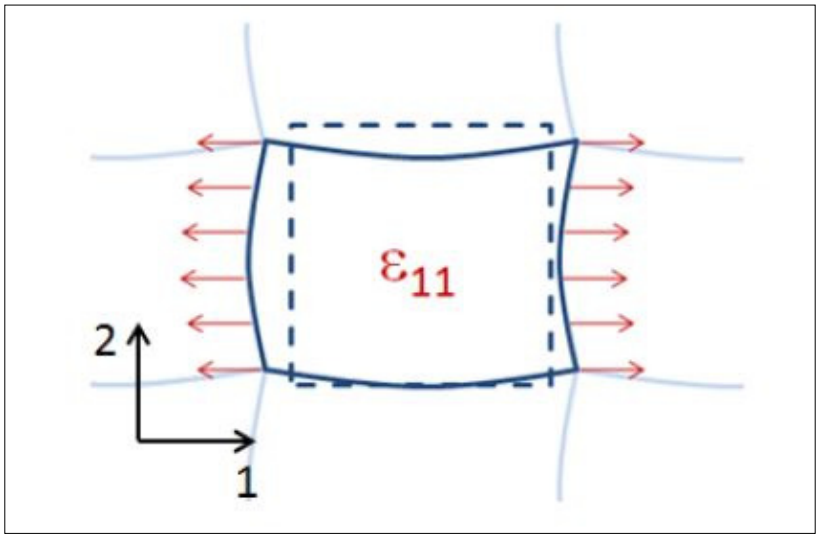


Figure 1.11 Periodic boundary conditions
From Digimat manual (2020, p. 641)

In various literary works, the utilization of periodic boundary conditions has successfully ensured the stability of the effective properties of Representative Elementary Volumes prior to the implementation of Dirichlet and Mixed boundary conditions (Kanit et al., 2003).

**Finite elements method**

The text discusses the increasing importance of computer-based design and analysis in high-technology fields. It significantly reduces the need for physical models and actual tests,

lowering design and development costs. This information can be found in various online resources related to the engineering and technology industries.

In addition, the finite elements homogenization approach is discussed, which aims to find a globally homogenous structure comparable to the initial material. According to (Kari, Berger, & Gabbert, 2007) (Moussaddy, 2013) this method has substantially increased over the last few decades due to the creation of sophisticated computer software.

These software-based simulation packages, including those that use the finite elements method and computer-aided design tools to model the geometry of engineering structures, serve as significant representations of the interaction between design and simulation. This can be found in a research paper by (Öchsner, 2016) discussing integrating different programs to facilitate the design and simulation process.

**The calculation of apparent properties**

In Digimat-FE software, the function "Automatic properties evaluation" allows the user to do the calculation for the elastic constants of the automatically generated volume.

The method that is used to calculate the apparent property tensor $\tilde{C}$ of a generated volume is applied by Digimat-FE according to what is done in Moussaddy's study (Moussaddy, 2013).

The apparent property tensor $\tilde{C}$ is calculated using the following equation:

$$\Sigma = \tilde{C} : K \tag{1.24}$$

With Σ (the macroscopic stress tensor), it is defined by:

$$\Sigma = < \sigma(x) > \mathrm{v} \tag{1.25}$$

(K) is the tensor for the macroscopic deformations which is calculated using Equation (1.26):

$$K =< \varepsilon(x) > \mathrm{v} \tag{1.26}$$

σ and ε represent respectively the local stress and the local deformation.

$$\Sigma =< \sigma(x) > \mathrm{v} = \frac{1}{V}\int_V \sigma(x)dV \tag{1.27}$$

$$K =< \varepsilon(x) > \mathrm{v} = \frac{1}{V}\int_V \varepsilon(x)dV \tag{1.28}$$

The "< >" presents the voluminal average of the discretized field.
For the discretized elements the calculation of the strain and stress tensors are defined as follow:

$$\Sigma =< \sigma_i > \mathrm{v} = \frac{1}{V}\sum V_i\sigma_i \tag{1.29}$$

$$K =< \varepsilon_i > \mathrm{v} = \frac{1}{V}\sum V_i\varepsilon_i \tag{1.30}$$

$V_i$ , $\sigma_\mathrm{i}$ and $\varepsilon_i$ represent respectively the volume, the constraint and the deformation associated with the finite elements i.

For better understanding of the calculation of $\tilde{\mathrm{C}}$ , Equation (1.31) can be written as follow:

$$\begin{bmatrix}\Sigma_{11}\\ \Sigma_{22}\\ \Sigma_{33}\\ \Sigma_{12}\\ \Sigma_{13}\\ \Sigma_{23}\end{bmatrix} = \begin{bmatrix}\tilde{\mathrm{C}}_{1111} & \tilde{\mathrm{C}}_{1122} & \tilde{\mathrm{C}}_{1133} & \tilde{\mathrm{C}}_{1112} & \tilde{\mathrm{C}}_{1113} & \tilde{\mathrm{C}}_{1123}\\ \tilde{\mathrm{C}}_{2211} & \tilde{\mathrm{C}}_{2222} & \tilde{\mathrm{C}}_{2233} & \tilde{\mathrm{C}}_{2212} & \tilde{\mathrm{C}}_{2213} & \tilde{\mathrm{C}}_{2223}\\ \tilde{\mathrm{C}}_{3311} & \tilde{\mathrm{C}}_{3322} & \tilde{\mathrm{C}}_{3333} & \tilde{\mathrm{C}}_{3312} & \tilde{\mathrm{C}}_{3313} & \tilde{\mathrm{C}}_{3323}\\ \tilde{\mathrm{C}}_{1211} & \tilde{\mathrm{C}}_{1222} & \tilde{\mathrm{C}}_{1233} & \tilde{\mathrm{C}}_{1212} & \tilde{\mathrm{C}}_{1213} & \tilde{\mathrm{C}}_{1223}\\ \tilde{\mathrm{C}}_{1311} & \tilde{\mathrm{C}}_{1322} & \tilde{\mathrm{C}}_{1333} & \tilde{\mathrm{C}}_{1312} & \tilde{\mathrm{C}}_{1313} & \tilde{\mathrm{C}}_{1323}\\ \tilde{\mathrm{C}}_{2311} & \tilde{\mathrm{C}}_{2322} & \tilde{\mathrm{C}}_{2333} & \tilde{\mathrm{C}}_{2312} & \tilde{\mathrm{C}}_{2313} & \tilde{\mathrm{C}}_{2323}\end{bmatrix}\begin{bmatrix}\mathrm{K}_{11}\\ \mathrm{K}_{22}\\ \mathrm{K}_{33}\\ 2\mathrm{K}_{12}\\ 2\mathrm{K}_{13}\\ 2\mathrm{K}_{23}\end{bmatrix} \tag{1.31}$$

The columns of the $\tilde{C}$ matrix are calculated based on solving the finite elements model six times, and by imposing six separate deformations (In the case of Dirichlet boundary conditions).

Each column of the matrix $\tilde{C}$ is solve as:

$$K^1 = \begin{bmatrix} \varepsilon \\ 0 \\ 0 \\ 0 \\ 0 \\ 0 \end{bmatrix}; K^2 = \begin{bmatrix} 0 \\ \varepsilon \\ 0 \\ 0 \\ 0 \\ 0 \end{bmatrix}; K^3 = \begin{bmatrix} 0 \\ 0 \\ \varepsilon \\ 0 \\ 0 \\ 0 \end{bmatrix}; K^4 = \begin{bmatrix} 0 \\ 0 \\ 0 \\ 2\varepsilon \\ 0 \\ 0 \end{bmatrix}; K^5 = \begin{bmatrix} 0 \\ 0 \\ 0 \\ 0 \\ 2\varepsilon \\ 0 \end{bmatrix}; K^6 = \begin{bmatrix} 0 \\ 0 \\ 0 \\ 0 \\ 0 \\ 2\varepsilon \end{bmatrix} \quad (1.32)$$

Each column of the flexibility matrix ($\tilde{S} = \tilde{C}^{-1}$) is determined by calculating the finite element model by imposing a tensile stress each time. The determination of the elastic constants is carried out by supposing that the material is orthotropic and isotropic planar. Therefore, the flexibility matrix $\widetilde{S}$, which is the inverse of the stiffness matrix, can be written as follow (Ngô, 2020):

$$\tilde{C}^{-1}=\tilde{S}=\begin{bmatrix} \frac{1}{E_1} & \frac{-\vartheta_{21}}{E_2} & \frac{-\vartheta_{31}}{E_3} & 0 & 0 & 0 \\ \frac{-\vartheta_{12}}{E_1} & \frac{1}{E_2} & \frac{-\vartheta_{32}}{E_3} & 0 & 0 & 0 \\ \frac{-\vartheta_{13}}{E_1} & \frac{-\vartheta_{23}}{E_2} & \frac{1}{E_3} & 0 & 0 & 0 \\ 0 & 0 & 0 & \frac{1}{G_{12}} & 0 & 0 \\ 0 & 0 & 0 & 0 & \frac{1}{G_{13}} & 0 \\ 0 & 0 & 0 & 0 & 0 & \frac{1}{G_{23}} \end{bmatrix} \quad (1.33)$$

From the previous matrix, the elastic constants (young's modulus E, Poisson's ratio $\vartheta$, shear modulus G of the material can be determined.

## 1.3 Performance evaluation of randomly oriented short fibers reinforce biocomposites by using numerical homogenization

Various industries rely on composite materials, making them a subject of recent research interest. However, developing these materials can take time and effort, prompting researchers to seek ways to reduce the time and cost required for experimental testing.

One approach is to predict the mechanical behavior of composites through techniques such as semi-empirical models, analytical homogenization, and numerical homogenization. These approaches are used to determine the effective properties of composite materials that contain random fibers. By employing these methods, researchers hope to streamline the development of composite materials and make them more accessible for use in different sectors.

### 1.3.1 Switchgrass fibers / PHBV-PBAT biocomposite tensile modulus

In a study conducted by the University of Guelph, the impact of fiber content on composite materials properties was investigated. The previous experimental investigation on composite materials reinforced with randomly oriented Switchgrass fibers indicated that as the composite material's fiber content increased, the composite material modulus gradually increased (Nagarajan et al., 2012). Therefore, the Tsai-Pagano model was utilized to compute the modulus values of randomly oriented fibers to estimate the theoretical tensile modulus of the manufactured composites.

Comparing the experimental and theoretical modulus of composites as a function of fiber volume showed that the increase in the measured modulus followed the same pattern as anticipated by the Tsai-Pagano model. However, the modulus derived from theoretical and experimental values were not sufficiently close, which necessitated the search for an analytical technique to obtain more accurate and realistic results to that of the experimental study (Nagarajan et al., 2012).

(Zou et al., 2010) also studied Miscanthus fibers, when he increased the length of the fibers, he noted that the flexural strength, and Young's modulus increased significantly with increasing fiber lengths from 1 to 5 cm, and then decreased significantly with increasing length from 5 to 10 cm. The aspect ratio of reinforcement material is a critical factor in determination the mechanical properties of the material (Zou et al., 2010). Figure 1.12 shows the effect of lengths of the fibers on mechanical properties.

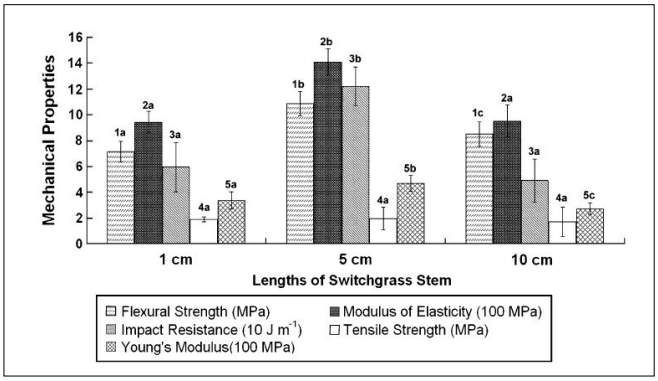


Figure 1.12 The effect of lengths on mechanical properties
From Zou et al (2010, p. 469)

### 1.3.2 Miscanthus fibers / PP biocomposite tensile modulus

Additional research was carried out to examine how randomly oriented natural fibers enhance composite materials mechanical properties. ÉTS University focused on studying the mechanical performance of composite F2, which included 30wt% of Miscanthus fibers by weight. Dhaouadi conducted experimental tests and obtained values for the tensile modulus of different composite materials, including the three composites tested in his study that varied in their reinforcing fibers content and type (Dhaouadi, 2018). The obtained tensile modulus values provided a foundation for further investigation of these composites. For composite F2, adding Miscanthus reinforcements resulted in an 18% increase in the matrix PP/POE flexural strength, as previously reported in the literature.

Finally, using the finite elements method and numerical homogenization, Dhaouadi created models of the three composite materials varying in weight and reinforcement type and obtained results close to the experimental findings using the commercial version of Digimat software.

### 1.3.3 Thermal effect on tensile modulus of biocomposites

Thermoplastic composites are becoming more prevalent in modern applications, particularly in the automobile sector. They offer a favorable cost-to-performance ratio, process ability, corrosion resistance, and ease of processing for complex geometries at high production rates. Many experimental studies investigated the effect of different temperatures on composite materials reinforced with randomly oriented short natural fibers. These studies confirmed a decrease in the modulus of elasticity when the temperature increased.

#### 1.3.3.1 Experimental study of the thermal effect on tensile modulus of PP

(Ragu, 2018) studied the mechanical properties of three composite materials with a polypropylene matrix as the focus of this research. One is reinforced with Biochar, another with Miscanthus vegetable fiber, and the third is a hybrid of the first two.

When increasing the temperature (37°C, 46°C, 57°C, and 66°C), It was noted that a decrease in modulus of elasticity with temperature rise for all three composites, as would be predicted. The fact that, regardless of temperature, the order of the materials confronting the distinct qualities stays constant suggests that temperature primarily affects their matrix and to a lesser extent, their reinforcements.

(Zhou & Mallick, 2002) also looked at how the heat affected the unfilled polypropylene matrix at (21.5°C, 50°C, 75°C, and 100°C). Unfilled polypropylene's elastic modulus and yield strength both dropped with rising temperature and rose with increasing strain rate. Figure 1.13 shows the tensile modulus of unfilled polypropylene at various temperature.

| Strain Rate ($min^{-1}$) | Temp (°C) | Parallel to the Flow Direction (L Direction) | | | Normal to the Flow Direction (W Direction) | | |
|---|---|---|---|---|---|---|---|
| | | Modulus (GPa) | Yield Strength (MPa) | Yield Strain (%) | Modulus (GPa) | Yield Strength (MPa) | Yield Strain (%) |
| 0.05 | 21.5 | 1.61 | 35.16 | 13.49 | 1.70 | 36.91 | 11.92 |
| 0.5 | | 1.76 | 38.23 | 9.76 | 1.85 | 38.82 | 9.23 |
| 5 | | 1.89 | 39.81 | 8.58 | 1.97 | 41.24 | 8.32 |
| 0.05 | 50 | 0.76 | 25.81 | 15.95 | 0.91 | 26.74 | 16.71 |
| 0.5 | | 0.88 | 28.02 | 12.10 | 1.01 | 29.32 | 13.65 |
| 5 | | 0.99 | 30.60 | 13.61 | 1.28 | 31.42 | 12.77 |
| 0.05 | 75 | 0.44 | 18.43 | 17.04 | 0.33 | 20.40 | 17.62 |
| 0.5 | | 0.51 | 20.46 | 14.46 | 0.40 | 22.14 | 15.07 |
| 5 | | 0.62 | 22.11 | 12.77 | 0.62 | 24.42 | 13.87 |
| 0.05 | 100 | 0.25 | 14.77 | 14.60 | 0.33 | 16.84 | 13.84 |
| 0.5 | | 0.38 | 16.29 | 12.55 | 0.41 | 18.35 | 12.20 |
| 5 | | 0.46 | 17.38 | 12.82 | 0.45 | 19.41 | 14.33 |

Figure 1.13 Tensile modulus of unfilled polypropylene at various temperature
From Zhou & Mallick (2002, p. 2453)

#### 1.3.3.2 Experimental study of the thermal effect on tensile modulus of the biocomposite Hemp/PP

In order to utilize the natural fibers as reinforcement in plastic composites, it has been observed by (Ho & Ngo, 2005) that temperature and humidity have an influence on the tensile behavior of Hemp fibers. Tensile strength, initial modulus, and elongation at rupture of untreated hemp fibers were measured and compared in ambient air and in water at various temperatures (23°C, 40°C, 60°C, 70°C, and 80°C). They found that the tensile strength and initial modulus of Hemp fibers decrease with increasing temperature in ambient air.

Keeping in mind that Hemp is a natural fiber that contains cellulose-lignin fibers, it is made up of many cylindrical cells that are bonded together. Each cell has a void space in the center. The cell wall is a composite material. Spirally oriented cellulose bands reinforce the hemicellulose and lignin matrix.

In order to verify the effect of heat on natural fibers, (Ho & Ngo, 2005) conducted a study on Hemp fibers, and it was confirmed that the tensile modulus of the fibers decreased when the

temperature increased. To assess the influence of temperature on the tensile properties of hemp in the air, data of the initial modulus are plotted in Figure 1.14.

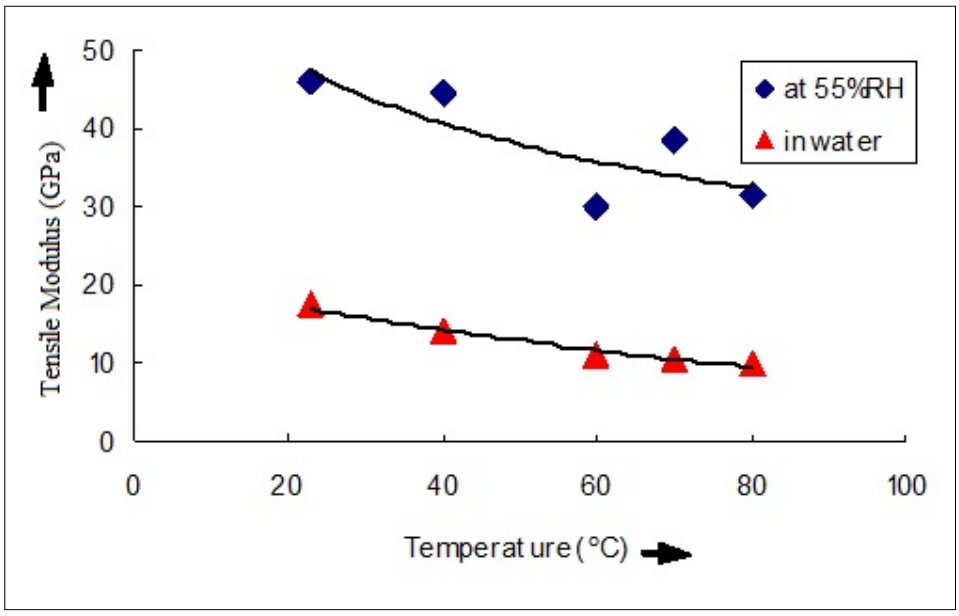


Figure 1.14 Modulus-Temperature curves of Hemp fibers at 55%RH and in water
From Ho & Ngo (2005, p. 9)

## 1.4 Objective of the study

Composite materials are increasingly being used as an alternative to traditional materials, focusing on those derived from natural sources. The new regulations to reduce greenhouse gas emissions mean that businesses in this sector must develop new materials. Furthermore, environmental concerns are also driving a move away from fossil fuels. In this context, there is interest in using plant-based reinforcements instead of synthetic ones, leveraging their low cost, biodegradability, lightweight, and renewability.

Previous studies have shown that certain biocomposites made up of polymers and natural fibers. This study builds on earlier work by (Nagarajan, 2012) and (Dhaouadi, 2018), the aim is to model the tensile modulus of two different biocomposite: the first composed mainly of PHBV/PBAT matrix reinforced with randomly oriented short Switchgrass fibers and the other

composed of a polypropylene matrix reinforced with randomly oriented short Miscanthus fibers.

As for the investigation of the effect of temperature rise on biocomposite materials, it was based on the investigations of (Ho & Ngo, 2005), (Zhou & Mallick, 2002), and (Ragu, 2018) to model the behavior of the polymer matrix and Hemp fibers at high temperature.

The study has three main objectives.
-First, it aims to validate the possibility of numerical modeling for composite materials by comparing results with earlier empirical and analytical studies.
-Second, it seeks to investigate how different fiber geometries affect the tensile modulus of biocomposites using numerical homogenization analysis and finite elements techniques. The goal is to create a model that can predict mechanical properties without extensive testing.
-Third, the study aims to model the impact of temperature on polymer matrix and on short natural fibers to predict the tensile modulus of biocomposite material under different temperature conditions.
Overall, this study can significantly improve the development of composite materials by allowing engineers to quickly and easily alter variables to achieve specific mechanical properties.

# CHAPTER 2

# FINITE ELEMETS SIMULATION

## 2.1 Numerical homogenization by the finite elements method

The primary goal of the finite elements homogenization approach is to identify a globally homogenous medium that is comparable to the initial composite (Kari, Berger, Rodriguez-ramos, et al., 2007). The components of this method are the generation of the RVE, the meshing of that volume, the computation of macroscopic stresses and deformations using the finite elements method, and lastly the determination of the apparent characteristics of the volume. A graphic explaining these procedures is shown in Figure 2.1.

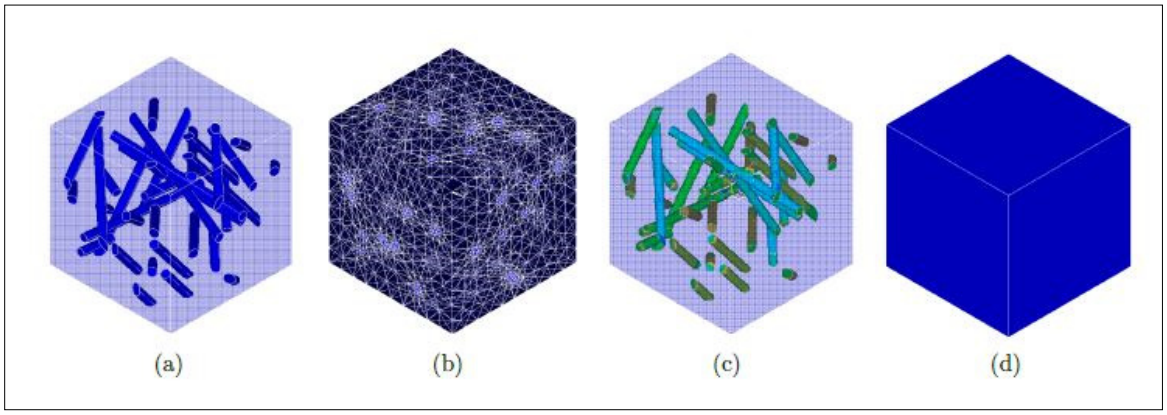


Figure 2.1 Fundamentals of numerical homogenization by the finite elements method From Moussaddy (2013, p. 70)

a) Generation of microstructures.
b) Mesh.
c) Digimat FE solution process.
d) Outcomes of numerical calculation.

E-Xstream Engineering creates and markets the package of the commercial software Digimat® for material suppliers and customers, a material modeling technology that expedites the production of composite materials and parts.

CAE engineers, materials scientists, and experts in the production of composite materials utilize Digimat solutions to predict accurately the nonlinear micromechanical behavior of complex multi-phase composite materials and structures. Digimat's users may develop and create composite materials and parts with remarkable efficiency in terms of both time and cost because of its effective and predictive capabilities.

In this study, Digimat-FE software is used to determine the tensile modulus of biocomposite materials. The process starts with entering the fundamental data for the phases to generate the microstructures, then moves on to the meshing of the phases. Digital solution process launches after to calculate the required mechanical properties, and finally the software presents the outcomes of the numerical solution in tables or curves. As it is shown in the workflow presented in Figure 2.2.

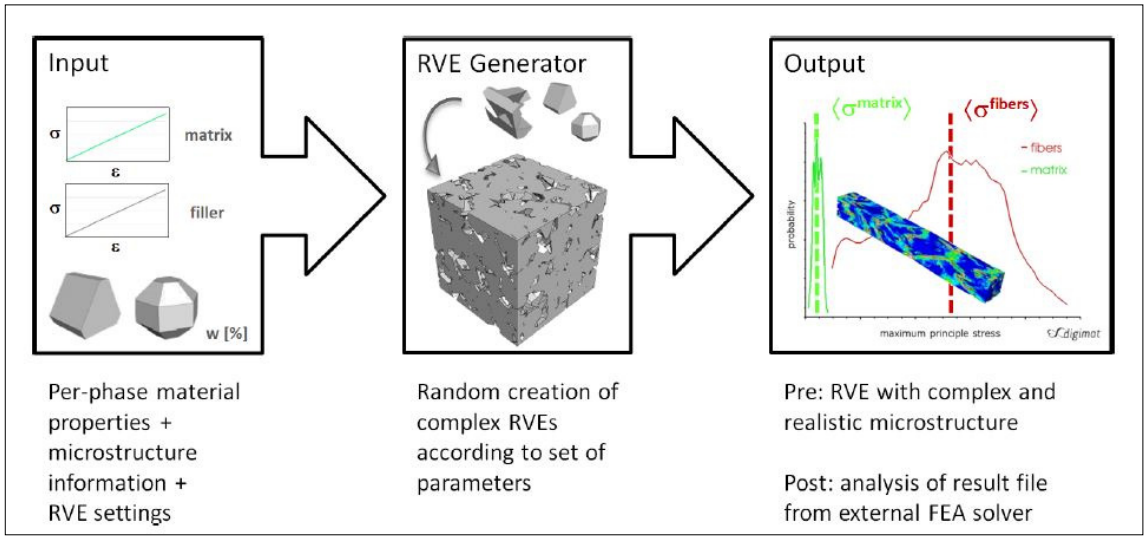


Figure 2.2 Digimat-FE workflow overview.
From Digimat manual (2020, p. 2010)

The apparent properties are the tensile properties of volumes less than the RVE, while the effective properties are those of the RVE (Huet, 1990). A modeling scale needs to be defined in order to create the actual composite properties. The scale used for this project is the microscopic scale, where the material is made up of precisely randomly oriented short fibers and matrix. This model does not account for the fiber-matrix interface.

There are additional assumptions used in the model that is being presented:

- The material exhibits isotropic transverse behavior (plane 1-2).
- The behavior of the fibers and matrix is isotropic.

Figure 2.3 shows the model to define phases.

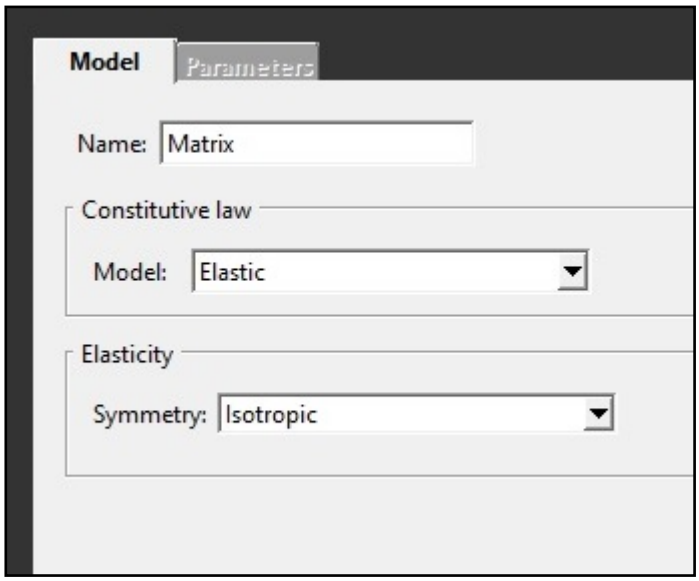


Figure 2.3 Defining the behavior of phases

## 2.2 Materials and input parameters

In this study, two biocomposite materials known as C1 and C2 are modeled. The first biocomposite material C1 was inspired by the experimental research conducted by (Nagarajan, 2012). The second one is named C2 was taken from the work of Dhaouadi (Dhaouadi, 2018). Keeping in mind that Dhaouadi did also a modelization on Digimat-FE of biocomposite materials.

The first biocomposite C1 is formed of the matrix (PHBV/PBAT) premix, which is marketed as ENMAT® 5010 P, and contains the following ingredients: 45wt% PHBV and 55wt% ECOFLEX® (PBAT) (Nagarajan, 2012). Second composite C2 contains a matrix made of polypropylene (PP) marketed by the trade name 1350N.

Switchgrass fibers reinforce the first composite. The length of the fibers after fabrication is around 1.58 mm and the fibers weight content is 30% (Nagarajan, 2012).
The Miscanthus short fibers length equals to 1.07mm; which are provided by COMPETITIVE GREEN TECHNOLOGIES.

Table 2.1 Composition of both biocomposite materials C1 and C2

| Biocomposite Material | PP (wt%) | PHBV/PBAT (wt%) | Switchgrass (wt%) | Miscanthus (wt%) |
|---|---|---|---|---|
| C1 | 0 | 70 | 30 | 0 |
| C2 | 70 | 0 | 0 | 30 |

Besides of the characteristics, the microstructure morphology of the constituent materials and the loading type of the model must be specified to the software in order to create the RVE.
The process of defining a material involves the following material characteristics as shown in Figure 2.3 and Figure 2.4 :

- The constitutive law, which is "Elastic" since it describes the properties of the elastic material.
- The behavior's isotropy or transverse isotropy is the second element. The fibers and matrix isotropy assumption should be chosen.
- Density values of the fiber and matrix.
- Young's modulus.
- Poisson's ratio.

Figure 2.4 shows the material characteristics to define phases.

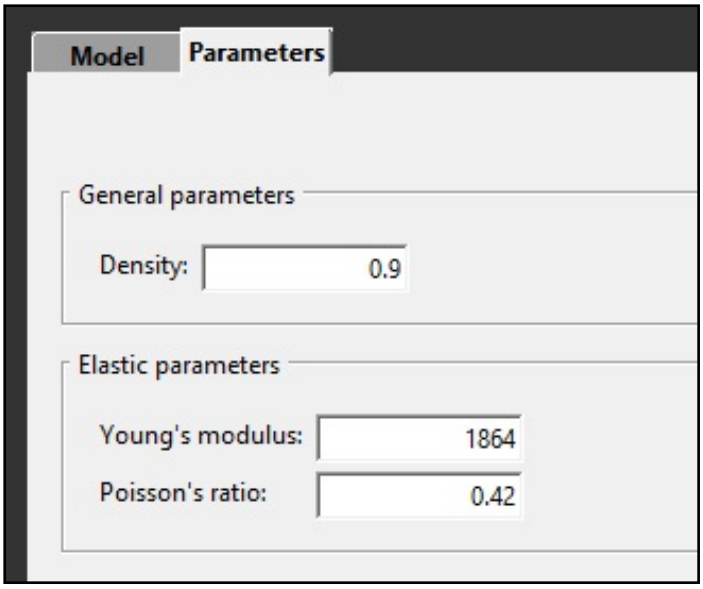


Figure 2.4 Mechanical properties inputs

### 2.2.1 Inputs for C1 biocomposite

In the C1 biocomposite, the fibers length is 1.58mm with a rectangular section (Nagarajan et al., 2012). Table 2.2 lists the mechanical properties of the Switchgrass fibers and the matrix (PHBV/PBAT).

Table 2.2 Inputs for C1 biocomposite

| Mechanical properties | Matrix (PHBV/PBAT) | Switchgrass |
|---|---|---|
| Young's modulus | 1.16 GPa (Nagarajan et al., 2012) | 9±2.7 GPa (Nagarajan et al., 2012) |
| Density | 1.23 g/$cm^3$ (Nagarajan et al., 2012) | 1.24 g/$cm^3$ (Nagarajan et al., 2012) |
| Poisson's ratio | 0.42 (Dhaouadi, 2018) | 0.2-0.3 (Miao et al., 2015)<br>0.22 (Dhaouadi, 2018) |

After defining the composite phases, it is necessary to incorporate the Switchgrass morphological features by uploading a "Parasolid" file that contains the fiber's form. The form of Switchgrass fibers is illustrated in Figure 2.5.

Solidworks® software provides the possibility to draw the morphology as a "Parasolid" form to use it with the modeling method.

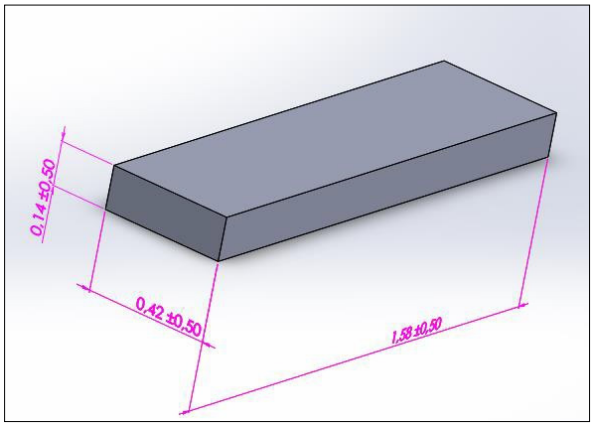


Figure 2.5 Switchgrass fibers morphology From Solidworks®

### 2.2.2 Inputs for C2 biocomposite

The second composite C2 uses 4 mm length of Miscanthus short fibers to reinforce the PP matrix. The essential parameters to calculate Young's modulus numerically are already determined in Dhaouadi's study (Dhaouadi, 2018). Mechanical properties of C2 biocomposite are shown in Table 2.3.

Table 2.3 Inputs for C2 biocomposite

| Mechanical properties | Matrix (PP) | Miscanthus |
|---|---|---|
| Young's modulus | 1.864 GPa (Dhaouadi, 2018) | 32.75 GPa (Bourmaud & Pimbert, 2008) |
| Density | 0.9 g/$cm^3$ (Dhaouadi, 2018) | 1.41 g/$cm^3$ (Muthuraj et al., 2017) |
| Poisson's ratio | 0.42 (Dhaouadi, 2018) | 0.25 (Miao et al., 2015) |

It has been reported that the fiber's length and the diameter reduced from 4mm to 1.07mm while the processing of the composite (Muthuraj et al., 2017). Therefore, in this modeling, the Miscanthus fibers are modeled as a cylinder form with a length of 1.07 mm and a diameter of 0.28 mm. The illustrated morphology of Miscanthus fibers is shown in Figure 2.6.

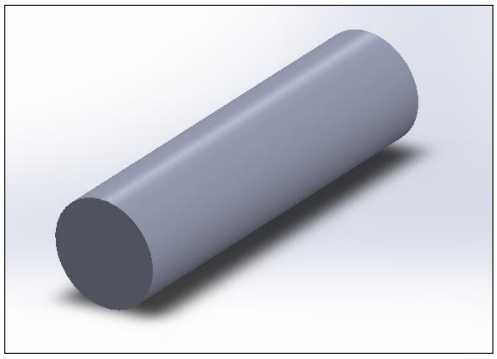

Figure 2.6 Miscanthus fibers morphology
From Solidworks®

Summarizing of what was mentioned, the process starts by defining the materials, including the isotropic behavior, mechanical properties, dealing with the interfaces between phases, and the morphology of the reinforcing fibers.

## 2.3 Calculation process

A three-dimensional (3D) representation of the microstructure is required in the homogenization technique.

The first step is defining the phases by entering the fundamental inputs for each phase. The second step is defining the microstructures in order to generate the RVE. Then generating the RVE that represents the studied material. After that, Digimat-FE requests the type of loadings, and it identifies what values are calculated for the results. Finally, the calculation process determines the affected properties of the studied composite.

### 2.3.1 The generation of the Representative Volume Element (RVE)

The difficulty of creating volumes with a high fibre volume content and a high aspect ratio (Length of the inclusion/diameter) is the key issue with this method. A finite element generation and computation program was utilized to produce the elementary volumes. With the necessary aspect ratio and fiber shape of the materials under study, the Digimat software enables the fibers to meet the volume content thresholds in the RVE. With the aid of the software Digimat-FE, it is possible to construct simple volumes with randomly oriented fibers. Digimat provides two techniques for producing RVE volumes with randomly oriented inclusions:

- User-defined volume fraction.
- Maximum packing algorithm.

These two options differ at the point when the generation stops. In the first algorithm, the generation stops once the volume fraction reaches the value that was set by the user, while the other algorithm stops for the maximum content of fiber generated.
The first algorithm was used in this research to generate the representative volume element, noting that based on Equation (1.7), the fiber weight content in the composite material was considered equal to the fiber volume fraction in this study.

Digimat-FE software works through the following steps in the generation of the inclusions (the fibers) in this study:

1. The generation starts with creating a single inclusion located at the center and follows the direction of the axis Z.
2. Then a similar inclusion with random orientation is generated (or inclusion with one direction the user had already defined).
3. A check for overlap is performed if interpenetration between inclusions is not permitted.
4. The algorithm goes back to step 2 in case there is an overlap between the inclusions.
5. Checking the terms of the minimum space permitted between the inclusions and the sufficient volume of the inclusions.
6. The algorithm continues to the following step if the conditions are verified; else, it returns to step number 2.
7. After that, the successful placement of the inclusion is recognized as having reached this milestone. The program now recalculates the new volume content that was attained, and compares it to the intended threshold. The algorithm ends when the required threshold is reached; otherwise, it goes back to step 1.

In order to compare with the results of Dhaouadi earlier research on the modeling of composite materials, the same size of RVE that was calculated by Dhaouadi is applied to generate the representative volume elements of C1 and C2 (Dhaouadi, 2018).
Volume creation can begin once the fibers and the matrix are defined in this instance.
Figure 2.7 presents the inputs for creating RVE geometries.

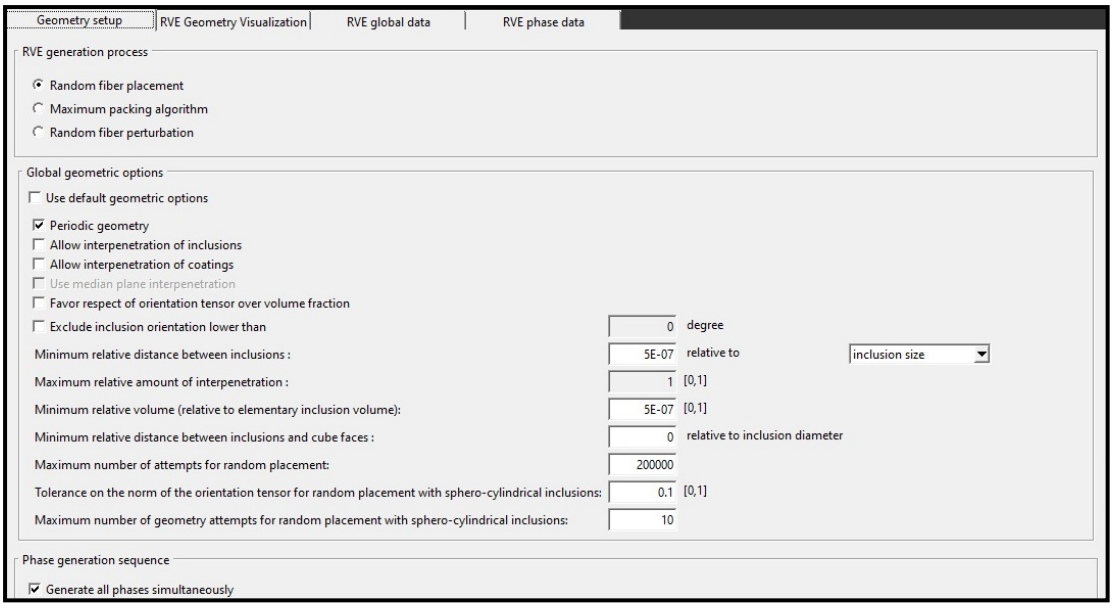


Figure 2.7 Geometries parameter's setup

For longer fiber, Digimat needs RVE with bigger size. This procedure might take hours to be completed, while in some cases it is not possible for the CPU to finish the task. It is preferable to decrease the distance between inclusions to get a desirable volume fraction.

Figure 2.8 presents the effective volume fraction calculated by Digimat.

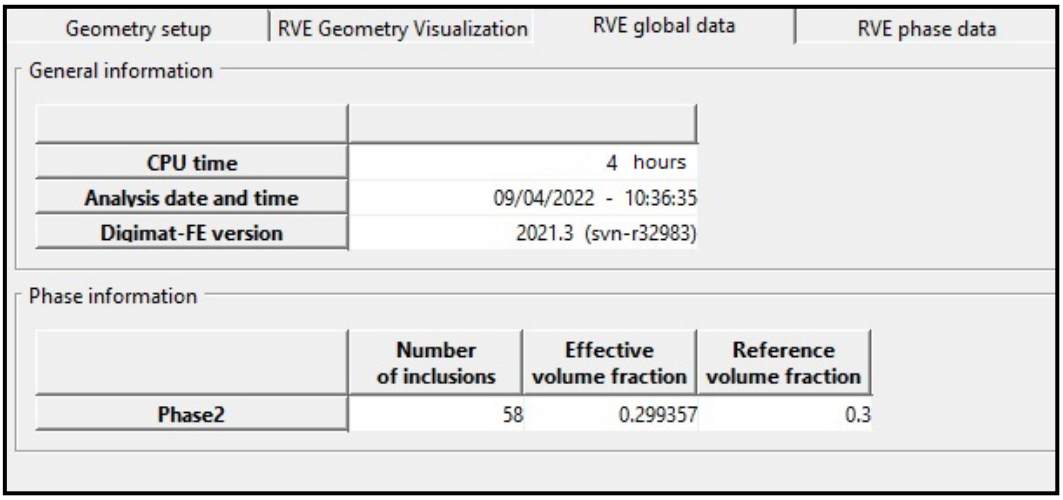


Figure 2.8 Parameters of generated geometries

Digimat software gives the possibility to choose between different methods to place the fibers in the generated RVE. Random fibers distribution can be produced in 2D or 3D.
Figure 2.9 illustrates 2D and 3D fibers distribution.

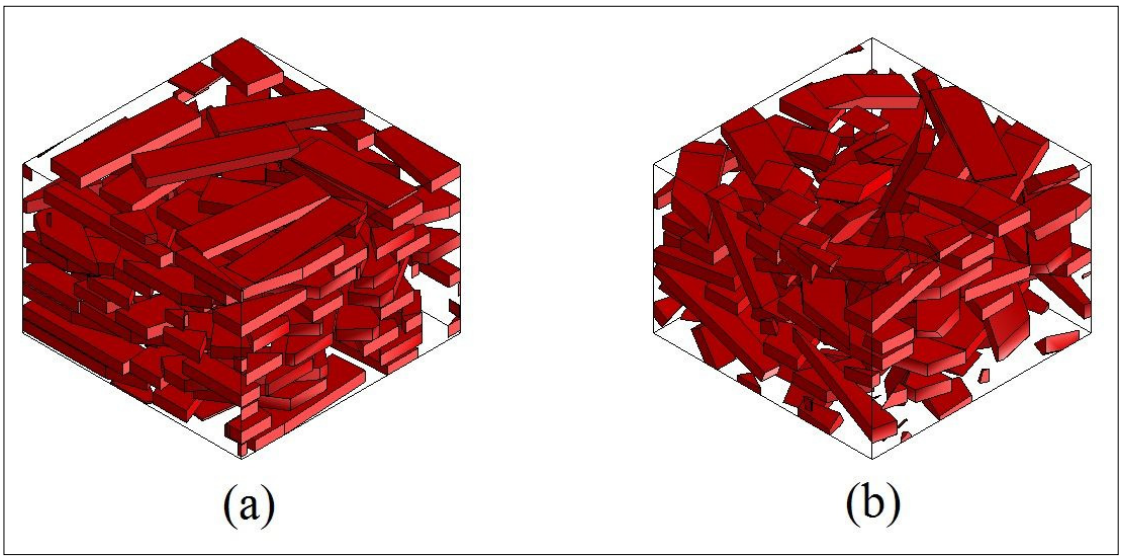


Figure 2.9 Fiber distribution in RVE
From Dhaouadi (2018, p. 78)

(a) Random fiber distribution 2D.
(b) Random fiber distribution 3D.

In order to compare with the work of (Dhaouadi, 2018), the generated RVE has the same 2D fiber distribution as Dhaouadi's RVE.

### 2.3.2 RVE meshing

Digimat-FE provides three distinct mesh types.

- Conforming (tetra).
- Non-conforming (voxel).
- Mesh cutting (tetra).

All RVEs, except those with inclusions in a curved spherocylinder shape, can use the conforming mesh. The non-conforming mesh is accessible for all RVEs, except those with void phases and inclusions with a curved sphero-cylinder shape. For inclusions with curved sphero-cylinder shapes, only the Conforming mesh algorithm is suitable. Figure 2.10 shows the inputs to generate the Conforming mesh used for the analysis in this work.

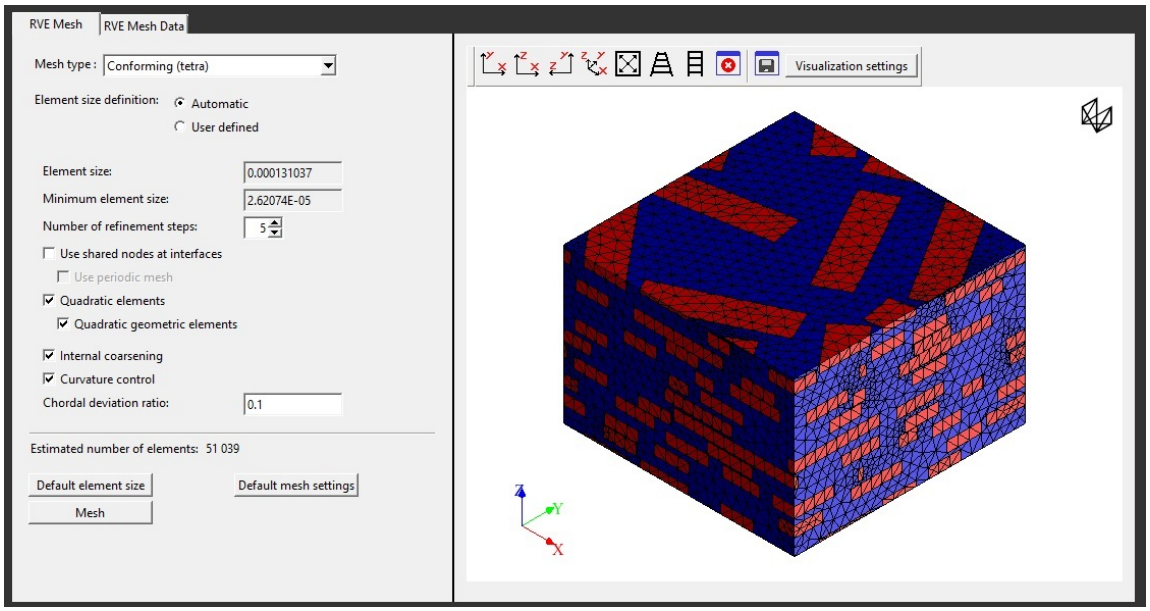


Figure 2.10 Digimat-FE mesh

Figure 2.11 shows the meshes for C1 biocomposite.

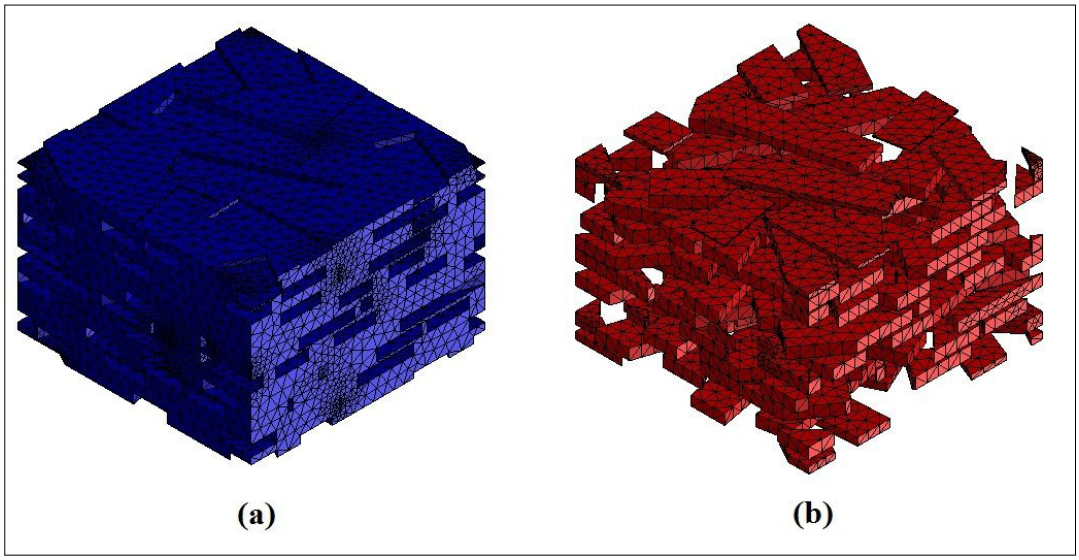


Figure 2.11 Meshed of phases for C1 composite.

(a) Meshed PHBV/PBAT matrix.

(b) Meshed SG fibers.

### 2.3.3 Loadings and boundary conditions

In Digimat-FE, there are four main types of analysis: mechanical, thermo-mechanical, thermal, and electrical. It is necessary to set suitable boundary conditions for each sort of analysis. There are several methods for applying these boundary conditions; Dirichlet type, Mixed, and Periodic type are each implemented in Digimat-FE.

The boundary conditions utilized have a major role in determining the elementary volume apparent qualities (Kanit et al., 2003). The boundary conditions applied for Dhaouadi's work are the periodic conditions, which require the realization of periodic geometries, which is not always possible with the Digimat, especially for large RVE sizes with a fiber volume percentage equals to 30wt%. Therefore, in the event that the implementation of the periodic geometries is not feasible, mixed boundary conditions are applied.


Figure 2.12 Boundary conditions and properties evaluation

### 2.3.4 Solution and results

Noting that by using the internal Digimat-FE mesher and solver make it easy to create the FE solver input file, to submit the FE job, to follow its progress, and to view the results after it is calculated by Digimat. The table of solver jobs contains a list of each FE task that is produced during the session. Solver job creation is shown in Figure 2.13.

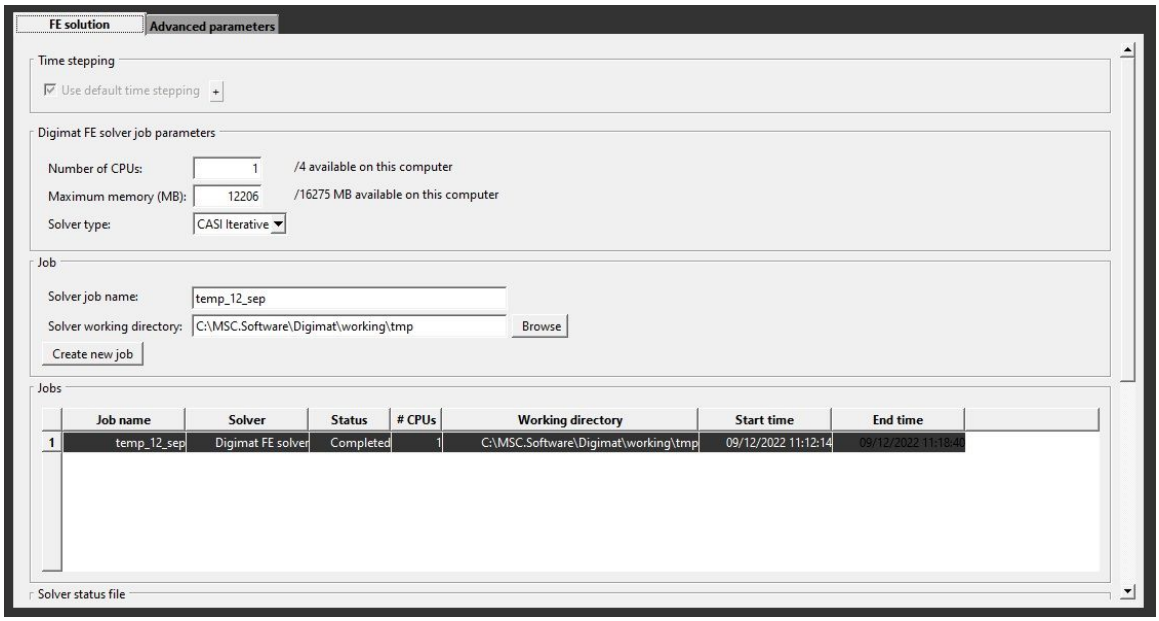


Figure 2.13 FE solution: solver job creation

## 2.4 Numerical modeling of the effect of the fibers geometries on tensile modulus of biocomposite materials

The primary goal is to know the effect of the fibers geometries on the tensile modulus of the biocomposite materials. For this, the tensile modulus is calculated when changing the form of the fibers, and then to take notes about the effect of this on the values of the modulus.
The studied parameters are the length, the cross section form, and the type of the fibers.

### 2.4.1 Modeling of the biocomposite C1

#### 2.4.1.1 Rectangular cross-section

The effect of the fiber's dimensions on the tensile behavior of biocomposite is evaluated by calculating the tensile modulus of five different fiber's length Table 2.4, and keeping the rectangular cross-section fixed. In the first case, the cross-section dimensions are fixed, only the length is changed.

Table 2.4 Length values of SG fibers

| SG fibers | $L_1$ | $L_2$ | $L_3$ | $L_4$ | $L_5$ |
|---|---|---|---|---|---|
| Length (mm) | 1.58 | 3.16 | 4.47 | 6.32 | 7.9 |

### 2.4.1.2 Circular cross-section

It is possible to consider an equivalent circular section of Switchgrass fibers, and to compare the results of the equivalent circular section. The diameter of the circular cross-section is found by equating the area of the rectangular cross-section and the area of the equivalent circular cross-section of the Switchgrass fibers. Figure 2.14 shows the equivalent circular cross-section and rectangular cross-section of Switchgrass fibers.

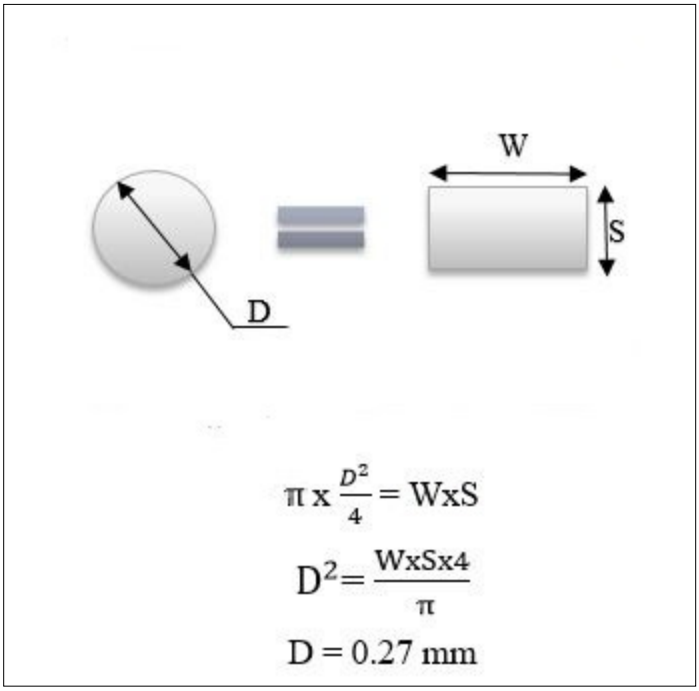


Figure 2.14 The diameter of the equivalent circular cross section

It is worthy to note that the volume of the fibers increases the RVE volume in order to keep the fiber's prescribed volume fraction of 30%.

### 2.4.2 Modeling of the biocomposite C2

The C2 biocomposite is reinforced with circular Miscanthus fibers, the effect of the fiber's length on the tensile modulus of this composite is studied. Table 2.5 shows the modeled lengths of Miscanthus fibers.

Table 2.5 Length values of MS fibers

| MS fibers | $L_1$ | $L_2$ | $L_3$ | $L_4$ | $L_5$ |
|---|---|---|---|---|---|
| Length (mm) | 1.07 | 2.14 | 3.21 | 4.28 | 5.35 |

## 2.5 Numerical modeling of the effect of temperature on tensile modulus of biocomposite materials

In this section, the capacity of numerical modeling to predict the behavior of biocomposites when heating occurs is discussed.

### 2.5.1 Modeling the effect of temperature on Polypropylene matrix

As pointed out in the literature, the temperature reduces the tensile modulus of the fibers and the polymer matrix. In order to calculate the tensile modulus of the biocomposite for different temperatures using Digimat software, it is necessary to know the thermal effect on the tensile modulus of the constituent materials of the biocomposite.

In order to comply with the temperatures in the study of (Ragu, 2018) which are 37°C, 46°C, 57°C, and 66°C, the values of the measured tensile modulus presented in Figure 1.12 has to be calculated by the interpolation in Equation (2.1) .

$$Y = \frac{(X - X_1)\,(Y_2 - Y_1)}{(X_2 - X_1)} + Y_1 \qquad 2.1)$$

Where:

X1,Y1 = First co-ordinates.

X2,Y2 = Second co-ordinates.

X= Target co-ordinate.

Y= Interpolated co-ordinate.

Table 2.6 presents the tensile modulus of polypropylene at 37°C, 46°C, 57°C, and 66°C that are used to calculate the tensile modulus of composite C2 by applying the interpolation on (Zhou & Mallick, 2002) results, to compare with the experimental data of (Ragu, 2018).

Table 2.6 Interpolated values of tensile modulus of PP matrix at different temperatures

| Temperature (°C) | 37 | 46 | 57 | 66 |
|---|---|---|---|---|
| $E_{pp\ (MPa)}$ | 1281 | 1004 | 776.4 | 643.2 |

.

### 2.5.2 Modeling the effect of temperature on the biocomposite Hemp/PP

Due to the absence of information related to the thermal effect on the mechanical properties of Miscanthus fibers, it is decided to use the thermal modulus of Hemp fibers, similar natural fibers, to study the effect of temperature on the tensile modulus of a bio-component similar to the components of biocomposite C2. This composite contains of 30% of Hemp fibers and 70% of PP matrix.Table 2.7 presents the tensile modulus of Hemp fibers extracted at 37°C, 46°C, 57°C, and 66°C in air obtained by (Ho & Ngo, 2005).

Table 2.7 Extracted values of tensile modulus of Hemp fibers at different temperatures

| Temperature (°C) | 37 | 46 | 57 | 66 |
|---|---|---|---|---|
| $E_{Hemp\ (MPa)}$ | 41584 | 38978 | 36412 | 34657 |

# CHAPTER 3

# RESULTS AND DISCUSSION

## 3.1 Validation of prior studies results

In order to validate the methodology, the results calculated by Digimat of two biocomposites C1 and C2 are compared with the ones that were calculated in literature.
Both biocomposite C1 and C2 are modeled in order to compare the results of this study with the ones that were obtained by Dhaouadi.

1- First, the biocomposite C1 is modeled, Table 3.1 shows the comparison between the values of tensile modulus E1 and E2 of C1 biocomposite taken from (Nagarajan, 2012) experimental work, with the results calculated by (Dhaouadi, 2018) by using Digimat, and the results calculated by Digimat in this study.

Table 3.1 Comparison between studied results and previous results of Dhaouadi for C1 biocomposite

| PHBV/PBAT+SG | E1 (MPa) | E2 (MPa) |
|---|---|---|
| **Experimental results from (Nagarajan, 2012)** | 2200 | 2200 |
| **Numerical results from (Dhaouadi, 2018)** | 2523.85 | 2539.25 |
| **Difference %** | 14.72 | 15.42 |
| **The numerical results of this study** | 2486.77 | 2450.4 |
| **Difference %** | 13.03 | 11.38 |

By comparing the results and the errors, it is notable that the current studied results are close to the previous ones reached by Dhaouadi; also, it is noticeable that the obtained results are more accurate by comparing the error.

2- As for the second biocomposite C2, it was modeled by Dhaouadi on Digimat software. The results of Digimat are shown in Table 3.2.

Table 3.2 Comparison between studied results and previous results of Dhaouadi for C2 biocomposite

| PP+MS | E1 (MPa) | E2 (MPa) |
|---|---|---|
| **Experimental results from (Dhaouadi, 2018)** | 3872 | 3872 |
| **Numerical results (Dhaouadi, 2018)** | 3619 | 3628 |
| **Difference %** | 6,35 | 6,3 |
| **The numerical results of this study** | 4089.67 | 4010.33 |
| **Difference %** | 5.6 | 3.5 |

Table 3.2 shows that the numerical results of C2 obtained in this research agree with the experimental and the calculated results by Dhaouadi, with more accuracy.
At this point, it is possible to ascertain the validity of using Digimat software to calculate the tensile modulus of biocomposite materials.

The accuracy of results can be attributed to the calculated fiber fraction value. For the RVE in this study, 30% of this of the fiber volume content value is reached where is Dhaouadi was able to reach only 29.5%.

## 3.2 The influence of fiber geometries on the tensile modulus of biocomposite materials

Regarding composite materials development, the influence of fibers geometries on the mechanical properties of composites is investigated in this study. It is known that by increasing the fiber geometry parameters, some mechanical properties of the composite material could be improved as shown in the literature (Zou et al., 2010). This behavior was modeled to verify the results by using Digimat-FE software.

### 3.2.1 Modeling C1 biocomposite

- **The influence of SG fibers length on the tensile modulus of C1 biocomposite with rectangular cross-section**

C1 biocomposite reinforced with rectangular cross-section of randomly oriented short Switchgrass fibers is modeled with different lengths of fibers. The RVE volume for 1.58mm fiber's length has the size of (3x3x2) mm, similar to the one in Dhaouadi's study. For longer fibers the RVE size was increased gradually in order to keep the content of fibers equals to 30%.

Table 3.3 Numerical results for the tensile modulus of C1 biocomposite with rectangular cross-section and different length values of SG fibers

| SG fibers | Length (mm) | E1 (MPa) | E2 (MPa) |
|---|---|---|---|
| $L_1$ | 1.58 | 2486.77 | 2450.4 |
| $L_2$ | 3.16 | 2539.33 | 2527.43 |
| $L_3$ | 4.47 | 2784.87 | 2746.47 |
| $L_4$ | 6.23 | 2781.57 | 2750.53 |
| $L_5$ | 7.9 | 2727.5 | 2726.63 |

Table 3.3 shows that the tensile modulus gradually starts to increase until the length of the fibers reaches the value of $L_3$. It is possible to call it the optimum length for fabrication. After that, any increase of fibers length over this value causes a degradation of tensile modulus. (Zou et al., 2010)

Here after is the explanation of (Zou et al., 2010) for this phenomenon;
The aspect ratio of the reinforcing elements is essential in determining composite mechanical properties. The high aspect ratio can facilitate stress transmission from reinforcements to matrix materials, consequently increasing mechanical characteristics. However, when SG stem lengths continue to rise, the dispersion of the stems over PP webs became less homogeneous due to the increasing size of the stems. Reduced homogeneity leads to a rise in flaws and a drop in elasticity modulus.

Figure 3.1 shows the convergence of E1 and E2. This is consistent with the isotropic characteristic of the composite material.

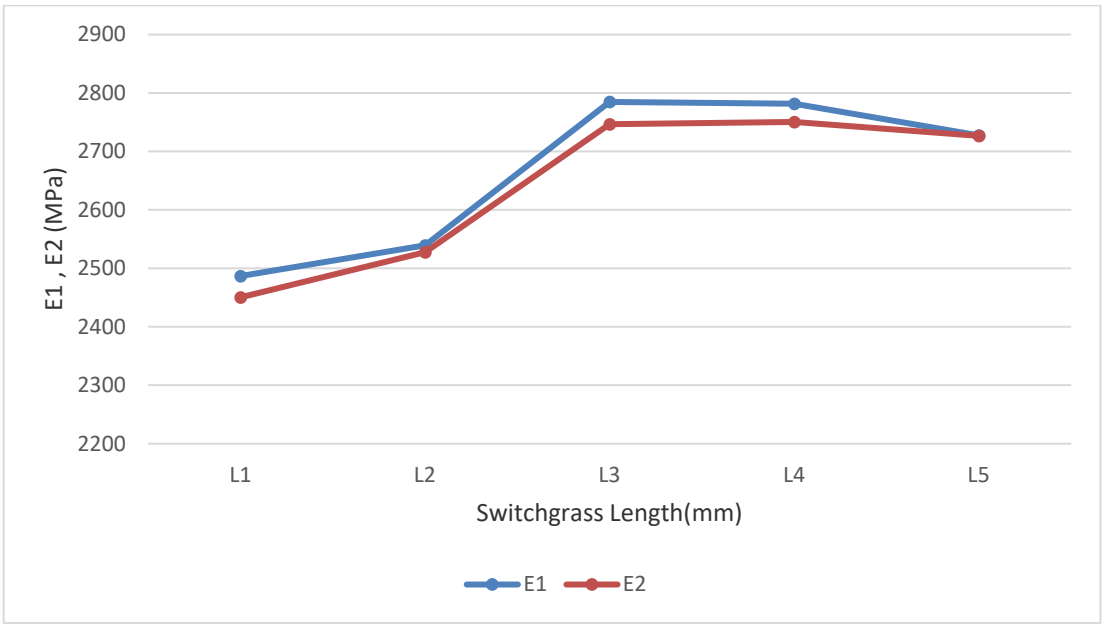


Figure 3.1 Numerical results for the tensile modulus of C1 biocomposite with rectangular cross-section and different length values of SG fibers

- **The influence of SG fiber's diameter on tensile modulus of biocomposite C1 biocomposite with circular cross-section**

A circular cross-section of Switchgrass fibers was proposed. This section is equivalent to the rectangular one that Dhaouadi experimentally studied. Depending on that, the equivalent diameter was calculated in the previous chapter. Based on this circular cross-section, biocomposite C1 with Switchgrass fibers is modeled to calculate the tensile modulus.

Table 3.4 shows the tensile modulus of C1 biocomposite for two equivalent cross-section (rectangular and circular).

Table 3.4 Comparison between the numerical results for the tensile modulus of C1 biocomposite with rectangular and circular cross-section of SG fibers

| SG fibers | E1 (MPa) | E2 (MPa) |
|---|---|---|
| **SG fibers with rectangular cross-section** | 2486.77 | 2450.4 |
| **SG fibers with circular cross-section** | 2121.67 | 2099.13 |
| **Difference %** | 14.68 | 14.33 |

The results indicate that E1≈E2 of the biocomposite material C1, which represents an isotropic behavior, corresponds with the assumption at the beginning of the modeling process.

Table 3.5 Numerical results for the tensile modulus of C1 biocomposite with circular cross section and different length values of SG fibers

| PHBV/PBMT+SG | Length (mm) | E1 (MPa) | E2 (MPa) |
|---|---|---|---|
| L1 | 1.58 | 2121.67 | 2099.13 |
| L2 | 3.16 | 2250.87 | 2292.43 |
| L3 | 4.47 | 2360.70 | 2387.3 |
| L4 | 6.23 | 2334.3 | 2317.8 |

Table 3.5 shows that the tensile modulus for C1 biocomposite reinforced with cylindrical Switchgrass fibers starts to increase, then it becomes stable after the length value L3 of Switchgrass fibers, this pattern was found previously for the rectangular SG fibers.

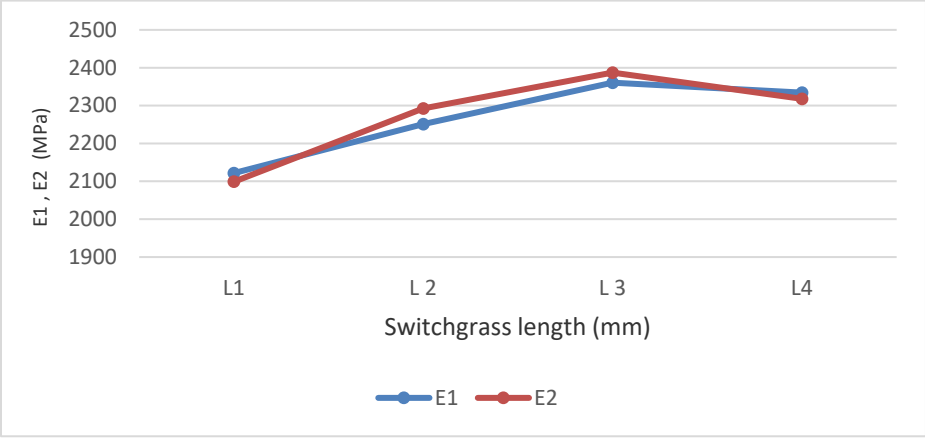


Figure 3.2 Numerical results for the tensile modulus of C1 biocomposite with circular cross-section and different length values of SG fibers

### 3.2.2 Modeling C2 biocomposite

- **The influence of MS fiber's length on tensile modulus**

It was previously noted that the length of the fibers is a factor affecting the mechanical properties of the composite materials; it is possible to verify that by modeling the composite C2. For this, the length of the Miscanthus fibers L is multiplied many times, and then the composite material is modeled at each value of the fiber length. Table 3.6 shows the numerical

results for the tensile modulus of C2 biocomposite with circular cross section and different length values of MS fibers.

Table 3.6 Numerical results for the tensile modulus of C2 biocomposite with circular cross section and different length values of MS fibers

| PP+MS | Length (mm) | E1 (MPa) | E2 (MPa) |
|---|---|---|---|
| **L1** | 1.07 | 4089.67 | 4010.33 |
| **L2** | 2.14 | 4308 | 4309.67 |
| **L3** | 3.21 | 4448.67 | 4438.67 |
| **L4** | 4.28 | 4553 | 4518 |
| **L5** | 5.35 | 4525 | 4598 |

Table 3.6 confirms that the tensile modulus increases when the length of the Miscanthus fibers increases, and then after a certain length becomes stable. The effect of the fiber's length and tensile modulus was discussed previously when modeling composite C1, and the results were similar to the ones obtained for composite C2.

## 3.3 The influence of temperature's rise on tensile modulus

The objective of this section is to investigate the effect of temperature on the tensile modulus of biocomposite material by using numerical modeling method. This behavior was investigated experimentally by Ragu (Ragu, 2018). He has measured the tensile modulus of C2 biocomposite at different temperatures.

As mentioned in Chapter 1, due to the lack of the information about the thermal effect on the exact constituent materials of C2 biocomposite, two scenarios are adopted to calculate the tensile modulus of the biocomposite at various temperatures.

### 3.3.1 The effect of temperature on tensile modulus of C2 biocomposite taking into account only the thermal effect on PP matrix

In this first attempt, the thermal effect of Miscanthus fibers is neglected. Only the tensile modulus of PP matrix at different temperature is taken from the work of (Zhou & Mallick, 2002) are used to evaluate the tensile modulus of C2 biocomposite at these temperatures.

Table 3.7 Numerical results of modeling the effect of temperature on C2 biocomposite taking into account only the thermal effect on PP matrix

| Tensile modulus | Temperature | | | |
|---|---|---|---|---|
| | 37°C | 46°C | 57°C | 66°C |
| **Experimental modulus of biocomposite C2** | 3.822 (GPa) (Ragu, 2018) | 3.574 (GPa) (Ragu, 2018) | 2.748 (GPa) (Ragu, 2018) | 2.215 (GPa) (Ragu, 2018) |
| **Experimental modulus of matrix (PP)** | 1.281 (GPa) Interpolation after (Zhou & Mallick, 2002) | 1.004 (GPa) Interpolation after (Zhou & Mallick, 2002) | 0.7764 (GPa) Interpolation after (Zhou & Mallick, 2002) | 0.6423 (GPa) Interpolation after (Zhou & Mallick, 2002) |
| **Numerical Modulus E1 of C2** | 3.234 (GPa) | 2.531 (GPa) | 2.178 (GPa) | 1.86 (GPa) |
| **Numerical modulus E2 of C2** | 3.186 (GPa) | 2.520 (GPa) | 2.160 (GPa) | 1.805 (GPa) |

Table 3.7 shows the results of numerical modeling of the effect of temperature rise on biocomposite materials . The results show the decrease in the tensile modulus of the constituent taking into account the thermal effect on the matrix. It is noted also that the value of the

modulus E1 and E2 of C2 biocomposite are very close, which supports the behavior of the isotopic material.

Both experimental and calculated tensile modulus of C2 biocomposite are plotted in Figure 3.3. The calculated values are lower than the experimental ones. This indicates that the temperature rise on the PP matrix can reduce the tensile modulus of C2 biocomposite. Keeping in mind that the PP studied by (Zhou & Mallick, 2002) might not be the same material as the PP in the C2 biocomposite.

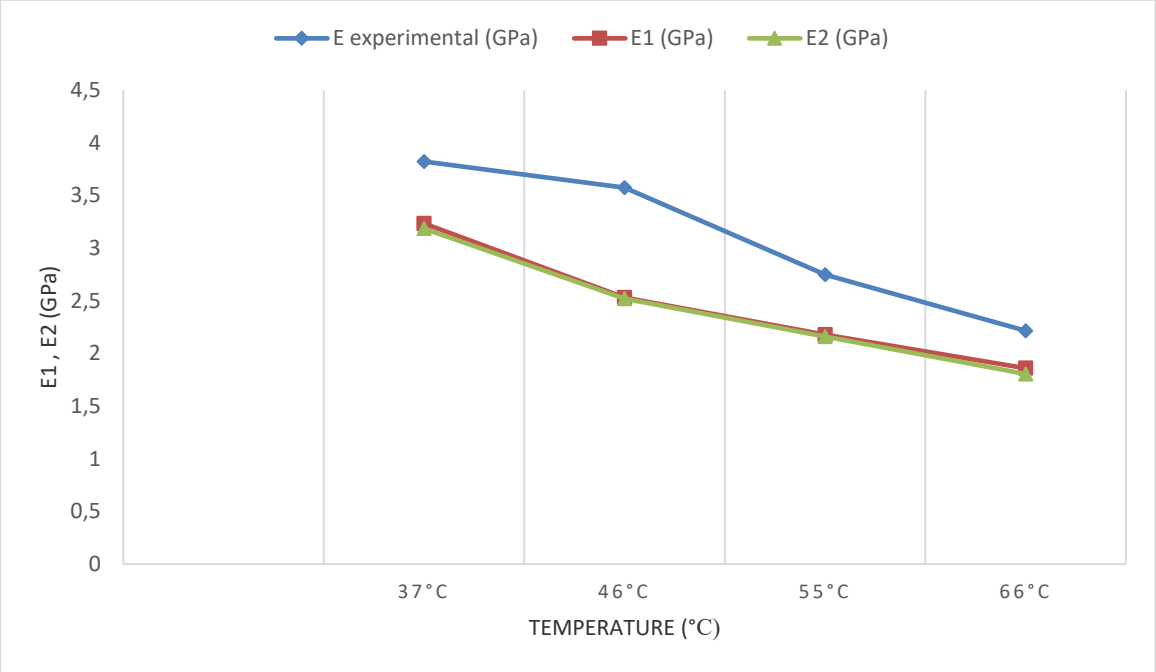


Figure 3.3 Numerical results of modeling the effect of temperature on PP matrix

### 3.3.2 The effect of temperature on the tensile modulus of the biocomposite (30wt%Hemp,70wt%PP).

In the second scenario, the temperature reduced tensile modulus of the PP matrix and the Hemp fibers are given to the software Digimat-FE to calculate the tensile modulus of the biocomposite. The results are presented in Table 3.8. It can be seen that the tensile modulus of

the studied composite at high temperature is affected mainly by the reduction of the tensile modulus of the PP matrix.

Table 3.8 Numerical results of modeling the effect of temperature on (Hemp/PP) biocomposite

| | Temperature | | | |
|---|---|---|---|---|
| | 37°C | 46°C | 57°C | 66°C |
| **Experimental modulus of biocomposite C2** | 3.822 (GPa) (Ragu, 2018) | 3.574 (GPa) (Ragu, 2018) | 2.748 (GPa) (Ragu, 2018) | 2.215 (GPa) (Ragu, 2018) |
| **Experimental modulus of matrix (PP)** | 1.281 (GPa) (Zhou & Mallick, 2002) | 1.004 (GPa) (Zhou & Mallick, 2002) | 0.7764 (GPa) (Zhou & Mallick, 2002) | 0.6423 (GPa) (Zhou & Mallick, 2002) |
| **Experimental modulus of Hemp fibers** | 41.584 (GPa) (Ho & Ngo, 2005) | 38.978 (GPa) (Ho & Ngo, 2005) | 36.412 (GPa) (Ho & Ngo, 2005) | 34.657 (GPa) (Ho & Ngo, 2005) |
| **Numerical modulus E1 of Hemp/PP biocomposite** | 3.347 (GPa) | 2.682 (GPa) | 2.183 (GPa) | 1.875 (GPa) |
| **Numerical modulus E2 of Hemp/PP biocomposite** | 3.355(GPa) | 2.643(GPa) | 2.197(GPa) | 1.893(GPa) |

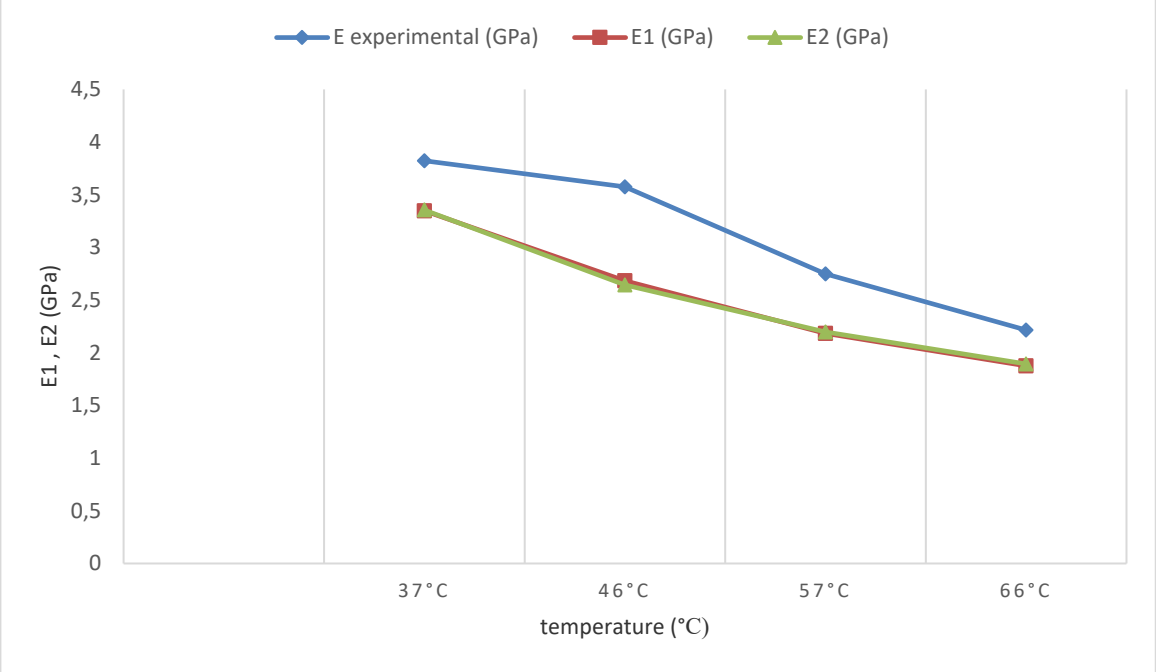


Figure 3.4 Numerical results of modeling the effect of temperature on (Hemp/PP) biocomposite and experimental results of the effect of temperature on (MS/PP) biocomposite

The numerical modeling of the temperature effect on biocomposite material yield the following conclusions:

- The tensile modulus of the matrix and the fibers decreases with the increase in temperature. This is what was found in previous experimental studies.
- The tensile modulus of biocomposite materials goes down as temperature rises. This is what prior experimental research discovered.
- The results of experimental tests are very close to numerical modeling results, with minor differences in the values between Hemp and Miscanthus fibers.
- The reduction of the tensile modulus of the biocomposite is affected mainly by the reduction of the PP matrix by temperature.
- Modeling the effect of temperature on biocomposite materials by using Digimat software was done successfully.

# CONCLUSION AND RECOMMENDATIONS

The scientific effort described here has added to understanding biocomposites using materials derived from renewable resources.

Numerical modeling is carried out on biocomposite materials reinforced with randomly oriented short natural fibers. The study is done by using numerical homogenization Digimat® software, which applies the finite elements approach to analyze the effect of fiber geometries and temperature on the tensile modulus of biocomposite materials. By performing the numerical modeling of composites C1, C2, and the composite (PP+30%Hemp). The results let to believe that:

- After validating the current work results by comparing them with the digital modeling results of Dhaouadi, it can be confirmed that it is possible to evaluate the tensile modulus of the biocomposites C1 and C2 using Digimat® software.
- When the length of the rectangular Switchgrass fibers increases, it leads to a higher tensile modulus.
- The essential factor in cylindrical fiber geometries is the ratio L/D, when the length of the fibers increases, the ratio L/D increases, and this leads to a higher modulus.
- After a certain value of fiber length, the tensile modulus becomes stable. The effect of the fiber length on the tensile modulus of biocomposites was discussed for both Miscanthus and Switchgrass fibers with cylindrical and rectangular cross-section, and it follows the same pattern. The results showed that the tensile modulus remains relatively constant after a certain value of fiber's length.
- The modulus of both matrix and fibers decreases with increasing temperature, AND consequently the modulus of the composite material reduces. The reduction in the tensile modulus of the biocomposite is principally due to the reduction of the matrix.

This search could be completed by modeling the effect of humidity on the tensile modulus of the matrix and the natural fibers to understand the impact of humidity on biocomposite materials. Based on this suggestion, it will be possible to predict the behavior of biocomposite

materials in different conditions of temperature and humidity, and this will help in choosing the optimal environmental conditions when testing and manufacturing biocomposites.

## BIBLIOGRAPHY


Bourmaud, A., & Pimbert, S. (2008). Investigations on mechanical properties of poly(propylene) and poly(lactic acid) reinforced by miscanthus fibers. *Composites Part A: Applied Science and Manufacturing, 39(9)*, 1444–1454. https://doi.org/doi: 10.1016/j.compositesa.2008.05.023.

Cox, H. L. (1952). The elasticity and strength of paper and other fibrous materials. *British Journal of Applied Physics*, *72*(3), 72–79.

Dhaouadi, T. (2018). *Caractérisation et modélisation des propriétés mécaniques des biocomposites à fibres courtes aléatoires par*. École de technologie supérieure.

E-Xstream. (2020). *Digimat manual* (Issue May). e-Xstream engineering.

Gibson, R. (2016). "Introduction," in Principles of Composite Material Mechanics. In *PRINCIPLES OF COMPOSITE MATERIAL MECHANICS* (4th Editio, Vol. 2). Taylor & Francis Group.

Gusev, A. A. (1997). Representative volume element size for elastic composites: A numerical study. In *Journal of the Mechanics and Physics of Solids* (Vol. 45, Issue 9). https://doi.org/10.1016/S0022-5096(97)00016-1

Halpin, JC. & Tsai, S. (1967). *Effect of environmental factors on composite materials, Air Force Technical Report AFML-TR 67-423*.

Halpin, J. C., & Pagano, N. J. (1969). The Laminate Approximation for Randomly Oriented Fibrous Composites. *Journal of Composite Materials*, *(3)*(4), 720–724. https://doi.org/10.1177/002199836900300416

Hill, R. (1963). Elastic properties of reinforced solids: Some theoretical principles. *Journal of the Mechanics and Physics of Solids*, *11*(5), 357–372. https://doi.org/10.1016/0022-5096(63)90036-X

Ho, T. N., & Ngo, A. D. (2005). Influence of temperatures and humidity on the tensile strength and stiffness of hemp and coir fibers. *5th Canadian International Composites Conference*, 1–11.

Huet, C. (1990). Application of variational concepts to size effects in elastic heterogeneous bodies. *Journal of the Mechanics and Physics of Solids*, *38*(6), 813–841. https://doi.org/10.1016/0022-5096(90)90041-2

K.Mohanty, A., Misra, M. & T.Drzal, L. (2006). *NATURAL FIBERS, BIOPOLYMERS, AND BIOCOMPOSITES : An Introduction* (L. K.Mohanty, A. K., Misra, M. & T.Drzal (ed.); 1st Editio, Vol. 1999, Issue December). CRC Press Taylor & Francis Group.

Kanit, T., Forest, S., Galliet, I., Mounoury, V., & Jeulin, D. (2003). Determination of the size of the representative volume element for random composites: Statistical and numerical approach. In *International Journal of Solids and Structures* (Vol. 40, Issues 13–14). https://doi.org/10.1016/S0020-7683(03)00143-4

Kanit, T., N'Guyen, F., Forest, S., Jeulin, D., Reed, M., & Singleton, S. (2006). Apparent and effective physical properties of heterogeneous materials: Representativity of samples of two materials from food industry. *Computer Methods in Applied Mechanics and Engineering*, *195*(33–36), 3960–3982. https://doi.org/10.1016/j.cma.2005.07.022

Kari, S., Berger, H., & Gabbert, U. (2007). Numerical evaluation of effective material properties of randomly distributed short cylindrical fibre composites. *Computational Materials Science*, *39*(1 SPEC. ISS.), 198–204. https://doi.org/10.1016/j.commatsci.2006.02.024

Kari, S., Berger, H., Rodriguez-ramos, R., & Gabbert, U. (2007). Computational evaluation of effective material properties of composites reinforced by randomly distributed spherical particles. *Composite Structures*, *77*, 223–231. https://doi.org/10.1016/j.compstruct.2005.07.003

Lu, Z., Yuan, Z. & Liu, Q. (2014). 3D numerical simulation for the elastic properties of random fiber composites with a wide range of fiber aspect ratios. *Computational Materials Science*, *90*, 123–129. https://doi.org/10.1016/j.commatsci.2014.04.007

Miao, Z., Phillips, J. W., Grift, T. E., & Mathanker, S. K. (2015). Measurement of Mechanical Compressive Properties and Densification Energy Requirement of Miscanthus × giganteus and Switchgrass. *BioEnergy Research, 8(1)*, 152–164. https://doi.org/10.1007/s12155-014-9495-8

Moussaddy, H. (2013). A new definition of the representative volume element in numerical homogenization problems and its application to the performance evaluation of analytical homogenization models [ECOLE POLYTECHNIQUE DE MONTREAL]. In *Thesis of Doctorat*. http://publications.polymtl.ca/1091/1/2013_HadiMoussaddy.pdf

Muthuraj, R., Misra, M., & Mohanty, A. K. (2017). Biocomposite consisting of miscanthus fiber and biodegradable binary blend matrix: Compatibilization and performance evaluation. *RSC Advances*, *7*(44), 27538–27548. https://doi.org/10.1039/c6ra27987b

Nagarajan, V. (2012). *Sustainable Biocomposites from 'Green' Plastics and Natural Fibers: INTRODUCTION* [The University of Guelph, Ontario, Canada]. http://hdl.handle.net/10214/3909

Nagarajan, V., Misra, M., & Mohanty, A. K. (2012). New engineered biocomposites from poly(3-hydroxybutyrate-co-3-hydroxyvalerate) (PHBV)/poly(butylene adipate-co-terephthalate) (PBAT) blends and switchgrass: Fabrication and performance evaluation. *Industrial Crops and Products*, *42*(1), 461–468. https://doi.org/10.1016/j.indcrop.2012.05.042

Ngô, A. D. (2020). *« Matériaux composites »* (Cours SYS857. Automne 2020. École de Technologie Supérieure.).

Öchsner, A. (2016). *Computational statics and dynamics: An introduction based on the finite element method* (pp. 1–485). https://doi.org/10.1007/978-981-10-0733-0

Ragu, J.-B. (2018). *Etude En Laboratoire De L ' Influence De La Granulometrie Sur Le Comportement*.

Suarez, S. A., Gibson, R. F., Sun, C. T., & Chaturvedi, S. . (1986). The influence of fiber length and fiber orientation on damping and stiffness of polymer composite materials. In *Experimental Mechanics: Vol. 26(2)*.

Sun, C. T., Gibson, R. F., & Chaturvedi, S. K. (1985). Internal damping of polymer matrix composites under off-axis loading. In *Journal of Materials Science* (Vol. 20).

Tsai, S., & Pagano, N. (1968). *Composite material workshop*.

Zhou, Y., & Mallick, P. K. (2002). Effects of temperature and strain rate on the tensile behavior of unfilled and talc-filled polypropylene. Part I: Experiments. [University of Michigan]. In *Polymer Engineering and Science* (Vol. 42, Issue 12). https://doi.org/10.1002/pen.11132

Zou, Y., Xu, H., & Yang, Y. (2010). Lightweight Polypropylene Composites Reinforced by Long Switchgrass Stems. *Journal of Polymers and the Environment, Springer*, 464–473. https://doi.org/10.1007/s10924-010-0165-4